Transportation Research Part D 136 (2024) 104482

Contents lists available at ScienceDirect

Transportation Research Part D

journal homepage: www.elsevier.com/locate/trd

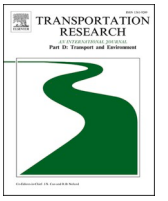

Unraveling hurricane Ian's Impact: A multiscale analysis of mobility networks in Florida

Jinpeng Wang, Yujie Hu *

Department of Geography, University of Florida, Gainesville, FL 32611, USA

ARTICLE INFO

Keywords:
Human Mobility
Mobility Networks
Spatial Networks
Network Motif
Hurricane Ian
Mobile Phone GPS Data

ABSTRACT

Understanding how human mobility patterns respond to natural disasters is crucial. This study investigates Hurricane Ian's impact on human mobility patterns and subsequent recovery in southwest Florida. Using privacy-preserving mobile phone GPS data, this research analyzes human mobility networks before, during, and after the hurricane, examining both macro and substructure (motif) levels. Additionally, this study investigates spatial variations in motifs over time, revealing localized connectivity patterns and adaptations in response to the hurricane's impact. The macroscale analysis shows a substantial decrease in mobility during the hurricane, leading to disruptions in connectivity and efficiency. However, the network demonstrated resilience by swiftly recovering post-hurricane. At the substructure level, different motifs exhibited varied responses, with densely connected motifs experiencing reductions in their percentage distribution, while less connected motifs showed increases. Moreover, there were shifts in the spatial distribution of motifs, which underscored vulnerabilities and adaptations within the mobility network. Understanding these dynamics during natural disasters can guide more targeted, spatially informed disaster management policies.

1. Introduction

Natural disasters present a formidable challenge to disaster management and preparedness. These events often lead to catastrophic impacts on human communities, infrastructure, and the environment (Choi et al., 2016; Gunderson, 2010; Sangha et al., 2020). Hurricanes, in particular, are known for their strong winds, heavy rainfall, and capacity for causing widespread damage. The extent of these impacts often depends on a range of factors, including the intensity and speed of the hurricane, as well as the level of preparedness in the affected areas (Mayer et al., 2008; Murnane and Elsner, 2012; Zhai and Jiang, 2014; Musinguzi and Akbar, 2021). In recent years, there has been an increasing interest in understanding how these disasters affect human behavior, particularly mobility patterns, due to the increasing availability of location tracking data (Han et al., 2019; Roy et al., 2019; Chen et al., 2020; Deng et al., 2021; Washington et al., 2024). Existing studies have highlighted the significant disruption hurricanes can cause to human movement patterns, including reductions in travel distance and frequency (Chen et al., 2020; Yum, 2021; Zhang and Li, 2022; Rajput and Mostafavi, 2023) and changes in travel direction (Han et al., 2019). This growing interest is driven by the need to improve disaster response and recovery efforts, as well as to build more resilient communities (Kates et al., 2006; Barnes et al., 2008; Brevard et al., 2008; Baum et al., 2009; Burton, 2014; Binder et al., 2015; Petkova et al., 2017).

One notable hurricane, Hurricane Ian, classified as a Category 5 storm, struck southwest Florida, causing widespread devastation.

* Corresponding author.
E-mail address: yujiehu@ufl.edu (Y. Hu).

https://doi.org/10.1016/j.trd.2024.104482
Received 2 April 2024; Received in revised form 11 September 2024; Accepted 20 October 2024
Available online 29 October 2024

Its intense severity led to significant damage, including extensive flooding, power outages affecting over two million residents, and urgent infrastructure reconstruction needs (Mazzei et al., 2022; Rafferty, 2022). Consequently, these outcomes resulted in substantial disruptions to mobility patterns within the affected areas, with 2.5 million people ordered to evacuate, and thousands trapped in the floods (Anderson, 2022; Gomez-Licon, 2022). Nevertheless, Hurricane Ian has received comparatively less attention in research despite its significant impact, and no studies have yet explored the extent of impact and recovery patterns within human mobility networks following Hurricane Ian. This understanding is crucial not only for effective disaster response but also for enhancing resilience and preparedness for future events.

Moreover, most existing studies focus on analyzing the impacts of natural disasters on human mobility patterns at a single scale, which limits their ability to fully capture the extent of both impact and recovery. This narrow focus overlooks the fact that mobility networks have distinct structural characteristics at different scales (Hsu et al., 2023). The physical characteristics of a hurricane—such as its landfall location, wind speed, and storm surge—coupled with differences in land use layout, road infrastructure, and the socioeconomic makeup of affected populations, means that mobility disruption levels are likely to vary significantly across different areas and scales. A multiscale approach is therefore essential, as it provides a fuller understanding of these diverse impacts, capturing both large-scale trends and localized vulnerabilities or resilience patterns.

This study aims to investigate the impact of Hurricane Ian on human mobility networks in southwest Florida and analyze the recovery patterns of these mobility networks following the hurricane. Using privacy-preserving mobile phone GPS data sourced from Cuebiq, this research constructs a series of mobility networks before, during, and after Hurricane Ian. Subsequently, structural properties of these networks are examined at both macro and substructure (motifs) levels. Examination of macroscale network metrics, such as network density, average path length, clustering coefficient, reciprocity, modularity, and robustness, sheds light on the hurricane's impact on the overall connectivity, cohesion, and resilience of the mobility network. At the substructure level, this study extracts and scrutinizes various types of network motifs, analyzing their frequencies, characteristics, and spatial distributions before, during, and after the hurricane's landfall. This analysis unveils impacts and recovery patterns at a finer substructure level that macroscale metrics are unable to capture.

This study makes several contributions to the growing field of research on human mobility dynamics during natural disasters. By centering on the relatively underexplored Hurricane Ian, a notably devastating hurricane, it addresses a notable gap in the literature by presenting empirical evidence from a distinct hurricane event. Unlike many existing studies that examine impacts at a single scale, the proposed multiscale approach captures both broad trends and specific localized effects, providing a thorough understanding of mobility impacts and recovery patterns across different scales. Furthermore, this research delves into the spatial patterns of motif dynamics, a dimension not previously explored in prior research. It examines the spatial distributions of each motif type and tracks their shifts throughout the hurricane. This approach is crucial for uncovering spatial variations in the magnitude of impacts and patterns of recovery, thereby enabling the development of targeted policy measures, particularly in areas with significant vulnerabilities in network structures at the substructural level.

2. Literature review

2.1. Human mobility patterns amid natural disasters

Natural disasters like earthquakes, hurricanes, floods, and wildfires profoundly affect human mobility (He et al., 2024). Traditionally, studies of human movement during these events, especially evacuations during hurricanes, have predominantly relied on surveys (e.g., Bowser and Cutter, 2015). These surveys investigate various aspects of evacuation decisions, such as destination, departure time, and factors influencing these choices (Tanim et al., 2022). While surveys provide detailed insights into individual behaviors, they are often resource-intensive and limited by spatiotemporal observation gaps and the absence of real-time location tracking (Yabe et al., 2022). Recently, passive GPS tracking data, such as mobile phone GPS data and social media geolocation data, has become one of the most prevalent sources for mobility analysis (González et al., 2008). GPS data enables detailed observation of mobility patterns across extensive geographic areas and over longer time periods (Zhang et al., 2014). Its longitudinal capability makes it superior in detecting regular movement patterns compared to traditional survey data, which is frequently constrained by recall bias and limited observation periods (Chen et al., 2016). In line with the scope of this research, the following review examines general human movement patterns derived from large-scale geolocation data, rather than focusing on specific trip types like hurricane evacuations.

Song et al. (2016) examined the impact of earthquakes and developed an effective model for predicting and simulating human mobility flows after natural disasters. Using large-scale GPS data along with other data sources, their study revealed that human mobility is more predictable and easier to simulate than previously thought. Tang et al. (2023) analyzed 1.32 billion mobile phone data records to examine human mobility resilience during the '720' Zhengzhou flood. Their study found that, despite overall reductions, mobility patterns remained largely stable and revealed distinct variations in resilience across different demographic groups. Anguelova et al. (2010) integrated fire behavior and pedestrian mobility models to assess wildfire risks to pedestrians in the U.S.-Mexico border region. Their framework proved effective in mapping high-risk areas and guiding emergency response strategies. Wang and Taylor (2018) analyzed 3.74 million geotagged tweets to examine the spatiotemporal dynamics between sentiment and human mobility before, during, and after the 2014 South Napa Earthquake. Their study revealed that sentiment declined with greater earthquake intensity and demonstrated a cointegrated relationship between sentiment and mobility patterns over time. Wang et al. (2017) analyzed geotagged Twitter data during a 2015 blizzard to examine the impact of severe winter storms on human mobility patterns. They found that both short and long trips were significantly disrupted, with noticeable deviations in mobility compared to normal

conditions. Maas et al., (2020) employed Facebook survey and mobility data to investigate population displacement during the 2019–2020 Australia bushfires, revealing gender disparities in evacuation behavior and access to protective equipment. Jia et al., (2020) examined population displacement patterns during California's mega-fires using Facebook Disaster Maps. It found that such a crowdsourced data platform effectively captured real-time population dynamics and provided valuable insights for disaster response and relief efforts. Fang et al., (2019) analyzed Weibo social media data to evaluate the impact and response to the 2016 Wuhan rainstorm, finding that social media is a valuable tool for real-time disaster assessment and management in China.

The study of human mobility during hurricanes, a critical natural hazard, has gained significant attention in recent years. Ahmouda et al. (2019) analyzed the impact of Hurricanes Matthew and Harvey on human mobility patterns across different U.S. regions. By harnessing Twitter data, their research unveiled a decrease in movement and activity space during the hurricanes. This study also shed light on the influence of user perceptions on Twitter during these events. Furthering this line of research, Han et al. (2019) delved into the spatiotemporal patterns of evacuation during Hurricane Matthew. Utilizing location data from Twitter, their analysis provided insights into evacuation behaviors, timing, and destinations. Notably, their findings suggested that human movements during evacuations adhere to a log-normal distribution, a significant contribution to understanding evacuation dynamics. Wang and Taylor (2015) expanded the scope of research by investigating the impact of severe tropical storms on human mobility in coastal cities using Twitter data. Their study encompassed movement patterns before, during, and after five major storms across eight urban areas. Their analysis revealed mobility disruptions attributed to the storms, showing a limited correlation with wind speed. Despite this, mobility continued to adhere to a power-law distribution, highlighting the resilience of the fundamental human mobility pattern despite such disasters. In a subsequent study, Wang and Taylor (2016) developed a computational model to simulate human mobility during hurricanes, taking Hurricane Sandy's impact on New York City as a case study. They proposed an agent-based model to simulate various emergency scenarios, aiming to support policymakers in decision-making processes for disaster response. They found that habitat fragmentation is one of the reasons why natural disasters have such influences on human activities. Deng et al. (2021) used over 30 million GPS records from Houston during Hurricane Harvey. Their study focused on relocation activities and revealed that while evacuation distance remained consistent across different neighborhoods, factors like race and wealth significantly influenced evacuation patterns. This research highlighted discrepancies in departure and return times and destination choices, offering valuable insights for disaster management and policy formulation. Fraser (2022) utilized Facebook mobility data and statistical modeling to analyze evacuation patterns during Hurricane Dorian. Their study found that linking social capital and community preparedness policies enhanced evacuation rates, whereas bonding social capital led to reduced evacuation.

As seen above, the influence of natural disasters on human mobility can be assessed using various metrics. Among existing studies, commonly employed metrics include changes in flow volume, which measure the fluctuations in mobility levels during disruptions (Gong et al., 2024; Li et al., 2024; Wang et al., 2024). Other commonly used metrics include changes in the radius of gyration and travel time. The radius of gyration measures the average distance traveled from a person's home base and helps reveal mobility constraints or evacuation patterns during disasters (Wang and Taylor, 2014; Wang and Taylor, 2018; He et al., 2024). Changes in travel time reflect disruptions in transportation networks, highlighting increased congestion or rerouting caused by damaged infrastructure (Solmaz and Turgut, 2017; Ilbeigi and Meimand, 2020; Jiang and Lin, 2022).

2.2. *Human mobility networks amid natural disasters*

Essentially, human movements, as spatial connections between locations, can be represented as networks. As a result, network analysis—a methodology for examining relationships and interactions within such networks—has become increasingly applied to human mobility research (Lee et al., 2022; Jing and Hu, 2024). For a comprehensive review of these studies, interested readers can refer to Barbosa et al. (2018). Thus, fundamental metrics for analyzing network structure—such as network density, clustering coefficient, average path length, modularity, and reciprocity (Newman, 2018; Jing and Hu, 2024)—are frequently employed to understand mobility network characteristics. Detailed descriptions of these metrics are provided in the following section.

Beyond examining the overall structural properties of a network, network analysis also offers the ability to analyze networks at multiple scales, including at the substructural level. Network motifs are substructures or subgraphs within complex networks that appear more frequently than expected in randomized networks (Milo et al., 2002). They function as the foundational components of complex networks that reveal important structural design principles across various systems, including biological, social, technological, and ecological networks (Milo et al., 2002). Network motifs are also employed in the analysis of human mobility networks. For example, Schneider et al. (2013) explored the underlying mechanisms of daily human mobility by analyzing thousands of individuals' movement trajectories as personal networks. They found that daily human mobility can be captured by 17 motifs, which are sufficient to represent up to 90 % of the population's movements. Cao et al. (2021) used mobile phone GPS data to analyze urban mobility networks, identifying individual travel patterns and their impact on urban structure and planning. They found that individual travel motifs, representing people's daily travel patterns, are structurally and spatially heterogeneous, indicating a wide variety of travel behaviors among the population. Su et al. (2020) developed a novel method for pattern recognition in human mobility by combining network motif analysis with activity sequence analysis. Using the 2017 California travel data, they identified distinct daily travel patterns and explored their correlations with various demographic groups and activities. Park and Zhong (2021) employed network motif analysis to investigate urban tourism patterns. They identified 12 key travel pattern topologies within city networks and examined how these patterns changed in relation to tourists' length of stay.

Although network analysis has many applications in human mobility studies, its use in examining human mobility during natural disasters remains relatively under-explored, with only a few studies investigating this specific area. For instance, Rajput and Mostafavi (2023) are among the few studies that have applied network analysis to human mobility during natural disasters. They used high-

resolution location data to build mobility networks in Houston during Hurricane Harvey, focusing specifically on the frequency distribution and characteristics of network motifs. Their study revealed that while macroscale properties indicated overall recovery, persistent disruptions continued to be evident at the substructure level. Similarly, Hsu et al. (2023) examined human mobility networks in eight Louisiana parishes impacted by Hurricane Ida. They used location tracking data to evaluate the resilience of mobility networks across macro, substructure, and micro scales. Their results underscored the diverse resilience characteristics observed in mobility networks across these scales, with macroscale measures showing faster recovery compared to substructure and microscale measures. This study highlighted the importance of employing a multiscale analytical approach to achieve a thorough understanding of network resilience in the context of natural disasters. While both studies provided insights into the resilience of network structures at the substructural level, they did not address the spatial dimension, which is crucial for understanding the spatial dynamics of these motifs.

3. Methods

3.1. Study area and data

This study focuses on Hurricane Ian, which made landfall in southwest Florida, notably affecting Lee and Charlotte Counties. At the county level, evacuation orders were issued for two areas within Charlotte County on September 26th and 27th, respectively. Meanwhile, in Lee County, evacuation orders were released on September 27th, less than 24 h prior to Ian's landfall. On the state level, the Governor of Florida mandated evacuations for the residents in 12 counties on September 27th. This order included Lee, Charlotte, Sarasota, and Collier Counties among others, affecting approximately 2.5 million people (Grant, 2022). Ian made landfall at Cayo

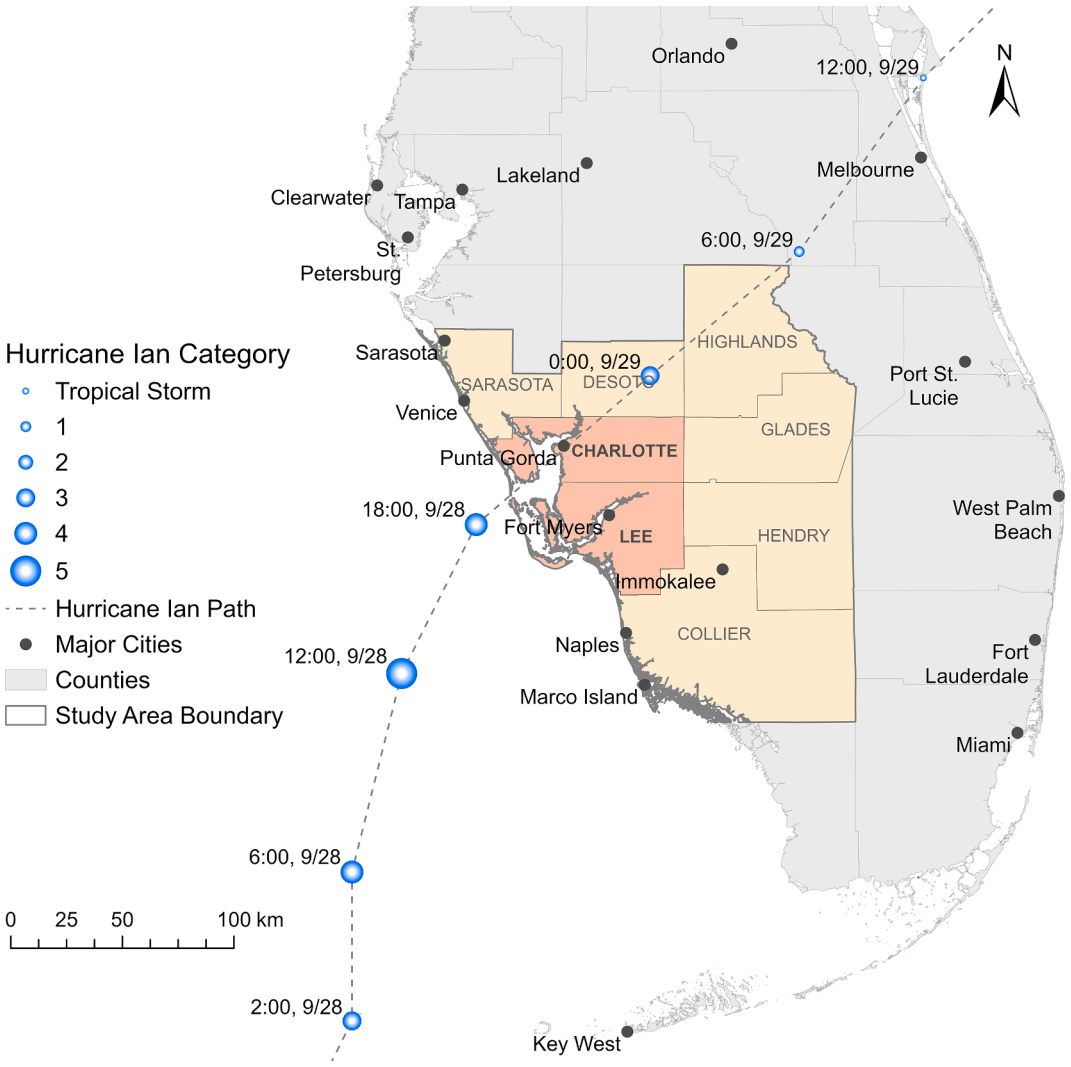

Fig. 1. Spatial distribution of the study area and the trajectory of Hurricane Ian.

Costa, Florida, in the afternoon of September 28th as a Category 4 hurricane. It proceeded to move northeast across the state, leaving Florida by the afternoon of September 29th before heading towards South Carolina (NOAA, 2022). Residents were ordered to stay or evacuate to other regions during the landfall period. Hurricane Ian is considered the costliest hurricane in the history of Florida and third costliest in the United States so far (Anderson, 2023). Therefore, the impact of Hurricane Ian presents a unique opportunity to examine disruptions in human mobility patterns following a significant natural disaster.

The study area encompasses the region most severely impacted by Hurricane Ian in southeast Florida, specifically Lee and Charlotte Counties, along with their six neighboring counties: Collier, DeSoto, Glades, Hendry, Highlands, and Sarasota (see Fig. 1). Notably, four of these adjacent counties rank among the top four origin and destination counties for travel to and from Lee and Charlotte Counties, highlighting their significance in the mobility dynamics during the hurricane. These counties are chosen deliberately to exclude the influence of other major metropolitan areas in Florida, such as Tampa to the north and Miami to the east. This strategy is implemented to minimize potential data distortions caused by broader mobility patterns associated with these larger urban centers, thus enabling a more focused and precise analysis of the localized impacts of Hurricane Ian.

The mobility data utilized in this research is sourced from Cuebiq, which gathers GPS data from mobile phones. Cuebiq acquires anonymous location data from nearly 70 million opted-in mobile devices across the United States through partner applications. Users voluntarily opt into the app's location services for research purposes, ensuring compliance with the General Data Protection Regulation (GDPR) and the California Consumer Privacy Act (CCPA). Users also retain the option to opt out of location services at any time. Cuebiq collaborates with over 220 mobile apps that integrate its proprietary software development kits (SDK). With data collection from approximately one in five smartphones in the United States, Cuebiq covers almost 20 % of the nation's population. The data collection process relies on the internal GPS hardware of devices. Cuebiq implements additional measures to safeguard privacy, including obscuring home locations at the census-block group level and excluding sensitive points of interest (POI) from the dataset. The data at the device level encompass recorded location information, comprising an anonymized individual ID, location coordinates, and corresponding timestamps (in seconds). Several recent studies have demonstrated the high validity of Cuebiq's mobile phone dataset (Pepe et al., 2020; Moro et al., 2021; Hsu et al., 2023; He et al., 2024).

Using locational information from the mobile phone dataset, trajectories of individual devices that both originate and terminate within the study area, spanning the eight selected counties, are extracted and included in this study. These trajectories are then aggregated into origin–destination (OD) flows at the census tract level (there are 422 tracts in the study area), forming directed and weighted mobility networks. In these networks, census tracts serve as nodes, aggregated mobility flows as edges, and flow volumes as edge weights. In particular, this study constructs a sequence of daily mobility networks spanning from September 1st to October 31st. This timeframe is selected to thoroughly encompass both the impact and recovery phases of Hurricane Ian.

To assess the representativeness of the mobile phone data, the number of mobile devices is compared to the population size (from the 2015–2019 American Community Survey) at the census tract level. As shown in Fig. 2, the high Pearson correlation coefficient of 0.9 demonstrates a strong alignment between the data and the population, indicating robust representativeness.

3.2. *Macroscale and substructure-scale network metrics*

The macroscale network metrics include the total edge weight, network density, average path length, clustering coefficient,

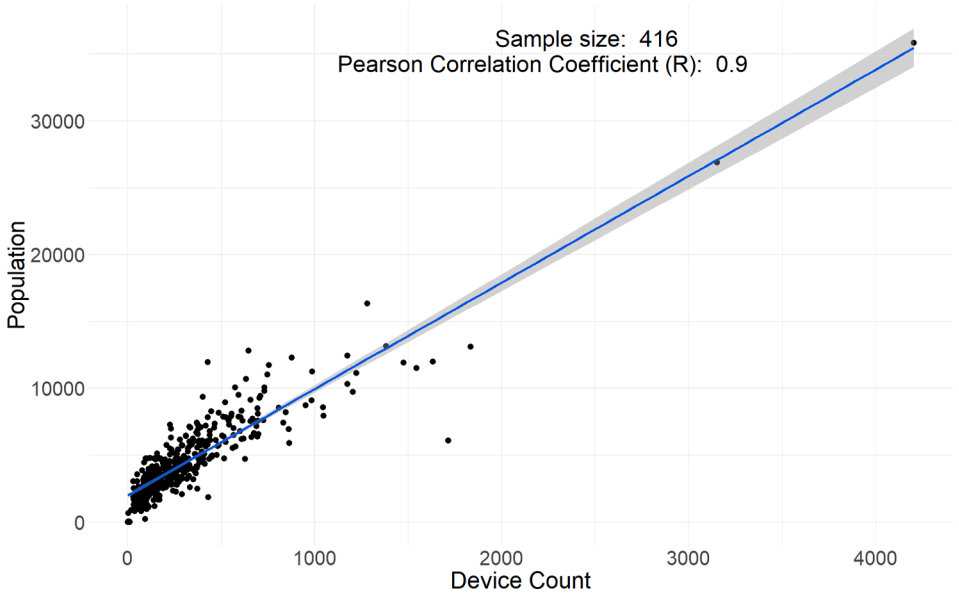

Fig. 2. Correlation between population size and mobile device count at the census tract level.

reciprocity, modularity, and robustness. These metrics are computed for each daily mobility network, providing insights into the overall structural changes in the mobility network during and after Hurricane Ian. They are chosen for their ability to detect key structural properties across various network types and their direct relevance to understanding mobility patterns. Table 1 provides detailed descriptions of several of these metrics. The total edge weight (W) is calculated by summing the weights of all edges in the network, providing a comprehensive measure of the cumulative volume of daily mobility flows and serving as an indicator of overall network connectivity and its variations in response to disruptive events such as hurricanes. Network density (ρ) is a measure calculated as the ratio of actual edges to potential edges in the network, with higher values indicating greater connectivity among nodes, thus reflecting a more tightly interconnected mobility system (Bhattacharya et al., 2023). The average path length (l) is a critical network metric that measures the average number of steps required to travel from one node to another across the network, providing insights into the network's efficiency and connectivity (Marinescu, 2017). A smaller value indicates greater network efficiency and connectivity, signifying more direct and easy mobility access between different areas. The clustering coefficient (C) measures the degree to which nodes in the network tend to cluster together, reflecting the local connectivity within the network (Bhattacharya et al., 2023). A higher clustering coefficient indicates stronger local ties, suggesting that nodes connected to a common node are likely to be directly connected as well, facilitating efficient communication and resource sharing within communities. This metric is crucial for evaluating community cohesion and localized mobility patterns, which are essential for effective disaster response and strategic urban planning. In a directed network, reciprocity (r) quantifies the likelihood of mutual connections between nodes, assessing the probability that if a node A has a directed edge to node B, then node B also has a directed edge to node A (Garlaschelli and Loffredo, 2004). A higher reciprocity value within our study indicates strong mutual mobility exchanges between tracts, suggesting that movements are reciprocally balanced, which is crucial for understanding the dynamics of bidirectional travel and enhancing connectivity within the mobility network. Network modularity (Q) quantifies the degree to which a network is segmented into distinct communities that are internally dense but sparsely connected to each other, serving as a measure of the network's natural division into clusters (Clauset et al., 2004). A high modularity score indicates that the network's structure is characterized by strong internal connections within communities and weaker connections between them, suggesting significant geographic or functional divisions within the mobility network. Network robustness is evaluated through two methodologies: random removal and degree-based removal of nodes, which test the network's resilience to disruptions (Callaway et al., 2000). The random removal method entails iterative trials where 5 % of the nodes are randomly eliminated, followed by an assessment of the largest connected component's size as a proportion of the total nodes after each removal. This process is repeated 100 times per network to minimize the effects of randomness. Conversely, the degree-based removal targets nodes with the highest degrees first, following a similar assessment procedure. Both methods provide insights into how well the network can maintain connectivity under random failures or targeted attacks, crucial for understanding its structural resilience.

At the substructure scale, this research turns to examining undirected 4-node network motifs, which represent small substructures within the larger network. There are 11 possible motifs in 4-node combinations. Note that only the combinations forming connected components are examined, as the aim is to understand the interconnections among these four nodes in each combination. These connected 4-node motifs can be categorized into six distinct types (see Fig. 3). These types include Clique (complete connection among the 4 nodes), Diagonal (similar to a Clique with one absent diagonal edge or a Loop with an additional diagonal edge), Loop (each node connects to 2 other nodes), Triangle (similar to a triangle with an extra node linked to one of the nodes), Chain (4 nodes connected as one long chain), and Hub-Spoke (one node connected to all other nodes). Given the complexity of analyzing all motifs across the six types from the 422 census tract nodes, 1,000,000 unique 4-node combinations are randomly sampled for each day's mobility network.

Table 1
List of macroscale network metrics used in the analysis.

Metric	Network Configuration	Formula	Description
Total edge weight (W)	Directed, weighted	$W = \sum_{e_{ij} \in E} W_{ij}$	E is the set of edges, and W_{ij} is the weight of the edge connecting nodes i and j.
Network density (ρ)	Directed, unweighted	For directed networks:$\rho = \frac{m}{n(n-1)}$	m is the number of edges, and n is the number of nodes in the network.
Clustering coefficient (C)	Directed, unweighted	For each node in directed networks: $C_i = \frac{\lvert\{e_{jk} : j,k \in N_i, e_{jk} \in E\}\rvert}{k_i(k_i-1)}$Average clustering coefficient for the whole network: $C = \frac{\sum_{i=1}^{n} C_i}{n}$	N_i is the neighborhood of node i (i.e., set of nodes with connection to i), e_{jk} is an edge from node j to node k, and E is the set of all edges in the network. k_i is the degree of node i, and n is the number of nodes in the network.
Average path length (l)	Undirected, unweighted	For undirected networks:$l = \frac{2\sum_{i \neq j} d(i,j)}{n(n-1)}$	$d(i,j)$ is the shortest path length between node i and j, and n is the number of nodes in the network.
Modularity (Q)	Undirected, unweighted	$Q = \frac{1}{2m}\sum_{ij}[A_{ij} - \frac{k_i k_j}{2m}]\delta(c_i, c_j)$	A_{ij} represents the adjacency between node i to node j (1 if connected and 0 if not), m is the number of edges in the network. k_i and k_j are the degree of node i and node j, respectively. c_i and c_j represents the community that node i and node j belongs to, respectively. $\delta(c_i, c_j)$ returns 1 if $c_i = c_j$ and 0 otherwise.
Reciprocity (r)	Directed, unweighted	For directed networks: $r = \frac{\sum_{e_{ji} \in E} \lvert e_{ij} \in E\rvert}{m}$	e_{ij} is an edge from node i to node j, E is the set of edges in the network, and m is the total number of edges.

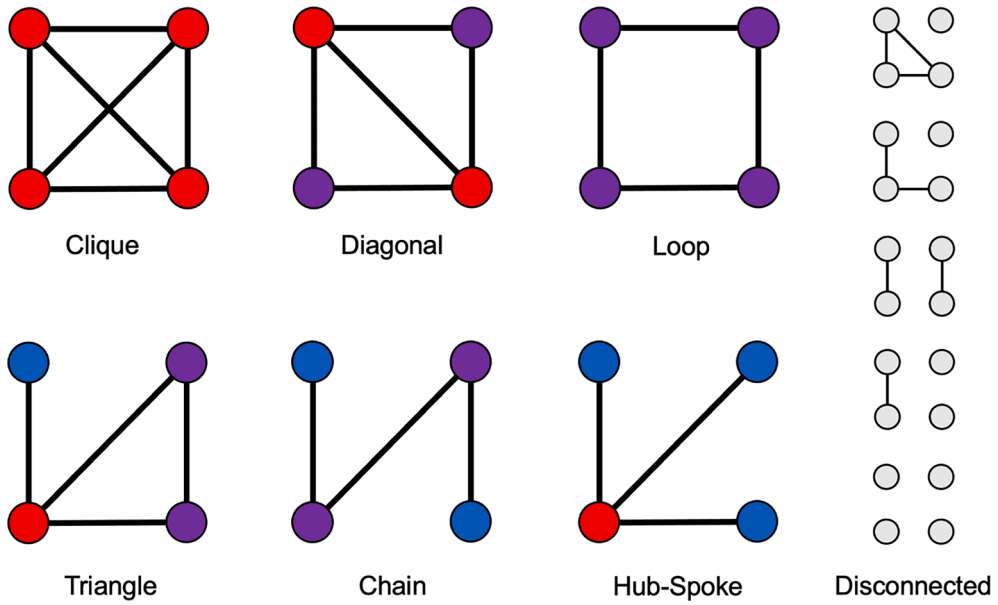

Fig. 3. Illustration of 4-node undirected motifs incorporated in this research, showcasing nodes color-coded according to their degree: red nodes with a degree of 3, purple nodes with a degree of 2, and blue nodes with a degree of 1. The 5 disconnected motifs are excluded in the analysis. (For interpretation of the references to color in this figure legend, the reader is referred to the web version of this article.)

To analyze the hurricane's impacts at the substructural level of the mobility network, this study calculates several key metrics for each motif type:

- **Frequency Distribution:** Indicates how often each motif type appears, helping to assess the prevalence of certain connectivity patterns before, during, and after the hurricane.
- **Average Edge Weight:** Measures the strength of connections within the motifs, which is crucial for understanding how mobility intensity changes during the hurricane.
- **Average Distance Between Nodes:** Reflects the spatial spread of the motifs, providing insights into how physical distance impacts network resilience during a hurricane.
- **Node Strength Difference:** The difference in node strength between the strongest and weakest nodes within a motif, indicating the balance of connectivity. A high difference may suggest connection vulnerability if key connections are lost.
- **Node Strength Dominance:** The ratio of the strongest node's strength to the total strength within the motif, highlighting how much one node dominates the connectivity. This is particularly important in motifs like Hub-Spoke, where the hub's dominance can be a point of failure.

Subsequently, the results are spatially mapped across the study area to illustrate the spatial distribution of motifs. Specifically, maps for three specific dates – one week preceding Ian's landfall (Sep 21st), the landfall date (Sep 28th), and one week post-landfall (Oct 5th) are generated for each motif type. These maps illustrate the spatial distribution dynamics of motifs throughout Hurricane Ian, providing a clear depiction of the spatial distribution of various motif types.

The mobility data are processed using Python's pandas package, then converted into spatial networks and analyzed with the NetworkX package to calculate mobility metrics and identify network motifs. Spatial maps of motif distributions are generated in ArcGIS Pro.

4. Results

4.1. Macroscale characteristics of human mobility networks

Fig. 4 provides a comprehensive overview of the changes in macroscale network metrics (described in Table 1) throughout the study period from September 1st to October 31st. A baseline for comparison is established by selecting the median values of each metric during the study period. Additionally, a 7-day moving average for these metrics is calculated to address the typical weekly patterns observed, as these measures often exhibit fluctuation between weekdays and weekends.

Before Hurricane Ian's impact, the total edge weight (W) exhibited a noticeable weekly pattern. However, a significant drop in mobility was noted starting on September 27th, one day before Ian's landfall, with W plunging nearly 90 % compared to the median level for that period on the day of landfall. Following the hurricane's impact, it took approximately two weeks for W to recover,

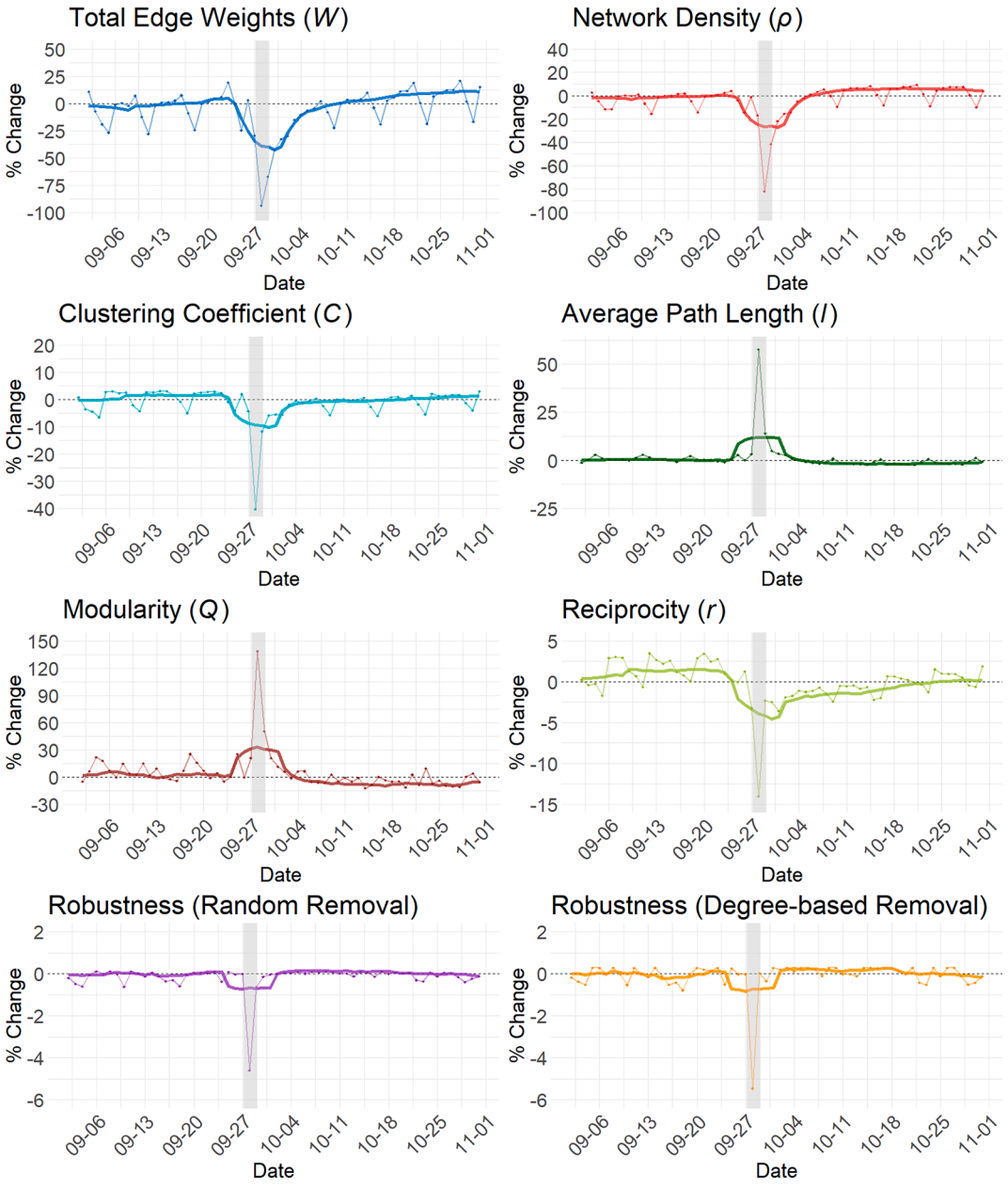

Fig. 4. Macroscale network metrics calculated for the mobility networks during the study period. Smoothed lines represent a 7-day moving average calculated to offset weekly differences, dashed lines depict the baseline value, and the grey bar indicates the period of Hurricane Ian's landfall.

eventually surpassing the baseline level.

Similar to W, network density (ρ) exhibited a comparable trend, initiating its decline the day before the hurricane's landfall and reaching a maximum drop of approximately 80 % compared to the baseline. However, the recovery of ρ was relatively swift, surpassing the baseline about a week after the impact. Given the relatively constant number of nodes throughout the period, this suggests a rapid rebound in mobility flows post-impact, despite the actual volume of mobility flows not immediately returning to normal levels.

The average clustering coefficient (C) decreased by roughly 40 % on the day Hurricane Ian made landfall, gradually recovering over the following week but not fully restoring to pre-impact levels. This partial rebound suggests lasting changes in the network's local connectivity. This sustained decrease in C implies enduring changes in local mobility patterns, possibly due to factors like infrastructural damage, changes in social behaviors, or a gradual, cautious return to normalcy.

The Average path length (l) showed less pronounced weekly pattern. During the hurricane, there was an approximate 55 % increase in l, which recovered to the baseline level within about 5 days. This increase indicates a substantial reduction in network connectivity during the hurricane, requiring more steps for node pairs to establish connections.

As Hurricane Ian made landfall, modularity (Q) increased by approximately 140 %, indicating a substantial shift towards more obvious community structures with fewer flows between different communities. This increase suggests a strong preference for individuals to travel within well-defined, closely-knit local areas, favoring familiar, contained routes—likely using pre-planned evacuation paths and local shelters—over broader, more expansive travel patterns. After recovering from the impact of the landfall, Q stayed at a level slightly lower than the baseline, indicating a weaker community structure compared to the mobility network before the landfall, possibly due to changes in the area's physical or social structures.

During landfall, there was a notable reduction in reciprocity (r) of approximately 15 %, indicating a shift towards unidirectional mobility patterns. This change likely signified a concentrated movement away from affected areas, with reduced or absent return flows as individuals prioritized evacuation or relocation to safer areas. The decline in reciprocal movement indicates that return trips were delayed, likely due to obstructed or damaged routes or because evacuees were staying in safer locations temporarily. It is noteworthy that reciprocity did not fully recover to pre-impact levels by the end of the study period. The sustained impact may indicate lasting alterations in mobility dynamics, possibly due to sustained changes in infrastructure, enduring shifts in residential or employment areas, or a more cautious attitude towards movement following the event.

Both robustness assessing methods yielded comparable results, indicating that network robustness remained consistent, except for a 5 % decline on the day of landfall. This slight decrease underscores that even during landfall, the average size of the giant component retained about 95 % of the entire network's nodes during the removal process. This highlights the network's robust resilience and interconnectivity, as evidenced by the minimal detachment of nodes from the giant component even during significant disturbances. The recovery process was relatively swift, taking approximately 2–3 days, compared to other macroscale metrics. The influence of weekly patterns on robustness metrics was almost negligible due to the network's high density, given that the size of the giant component typically approached the number of nodes in the entire network.

4.2. Substructural characteristics of human mobility networks

4.2.1. Motif frequency distribution and characteristics

Fig. 5 presents the frequency distributions of the six motif types identified from the sampled 1,000,000 4-node combinations during the study period. Across all six identified motif types, a distinct weekly pattern was observed, indicating the influence of weekly cycles on human mobility. Substantial variations in counts were noted among different motif types. Specifically, the Triangle and Chain types emerged as the most prevalent throughout the period. However, determining the most abundant motif type between the two was quite challenging due to their varying frequencies throughout the week. The Triangle type was more prevalent on weekdays, while the Chain type dominated on weekends. A parallel trend was noted for the Diagonal and Hub-Spoke types, both ranking as the second tier in terms of motif frequency. Specifically, the Hub-Spoke type was more common during weekends, while the Diagonal type appeared more frequently on weekdays. Despite these variations, both motif types maintained similar average counts.

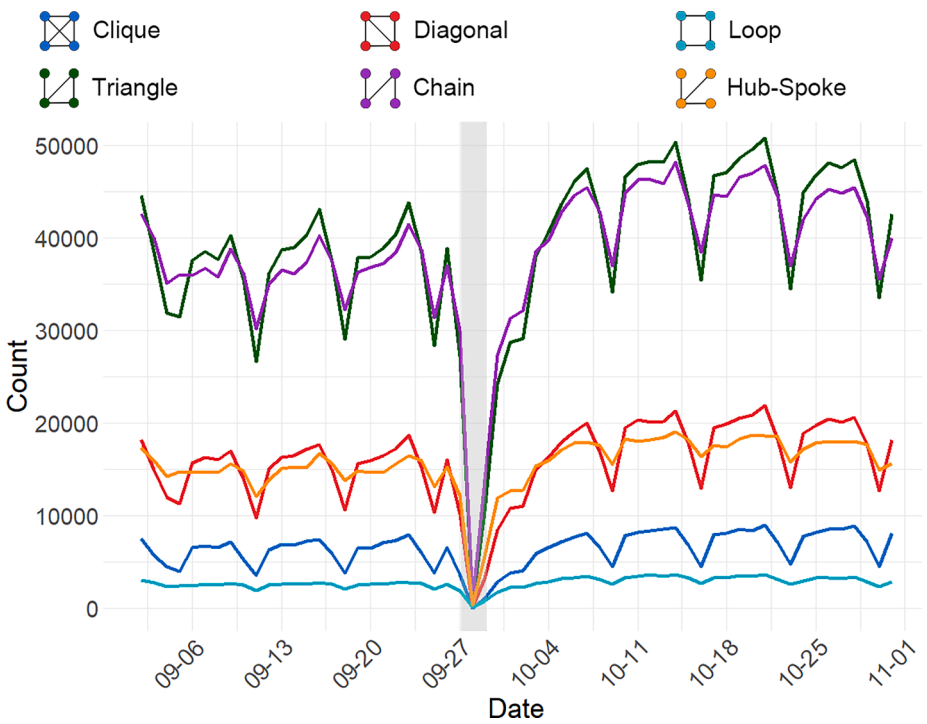

Fig. 5. Frequency distribution of the six motif types, with the grey bar indicating the period of Hurricane Ian's landfall.

It is important to note the structural differences among these motif types even though they exhibit similar counts within each tier group. For instance, the Triangle type consists of four edges, whereas the Chain type comprises three. Similarly, the Diagonal type encompasses five edges, in contrast to three edges of the Hub-Spoke type. Interestingly, the Clique type, characterized by complete connectivity, did not exhibit the lowest count throughout the study period. Instead, the Loop type, where all four nodes hold equal status within the motif but with lower connectivity, recorded the least frequency among all motif types. This observation is interesting as it suggests that fully connected motifs are not necessarily the least common type in mobility networks.

Fig. 6 illustrates the percentage shifts in the frequency distribution of each motif type among all motifs throughout the study period, with the baseline set as the median distribution of each motif type. The results unveiled notable patterns and fluctuations in response to Hurricane Ian's impact, highlighting the varying resilience of these motif types to this event. At landfall, substantial declines were observed in the percentage distribution of highly connected motif types, including the Clique and Diagonal types, which experienced reductions of approximately 80 % and 70 %, respectively. Nevertheless, these types quickly recovered, returning to baseline levels within approximately a week. The presence of a clear weekly pattern in these types underscores the impact of regular weekly cycles on these more complex, interconnected motif types within the mobility networks.

In contrast, the Loop type exhibited a different response to the hurricane's impact. Rather than experiencing a drop during Hurricane Ian, its percentage distribution increased above the baseline following the event, lasting for about three weeks before returning to the baseline level. The absence of a clear weekly pattern in the change of distribution for the Loop type suggests a distinct resilience or adaptability to the disruptive effects of the hurricane. Meanwhile, the Triangle type, which shares the same number of edges, showed a 40 % decrease in its percentage distribution during landfall, followed by a recovery to the baseline level within approximately one week. This pattern suggests a moderate level of impact and resilience in this motif type.

On the other hand, the two least connected motif types, Chain and Hub-Spoke, saw an increase in their percentage distribution during landfall, possibly indicating heightened evacuation and gathering behaviors. This observation is particularly notable as it contrasts with the more connected motif types, which experienced substantial decreases in their percentage distribution during landfall.

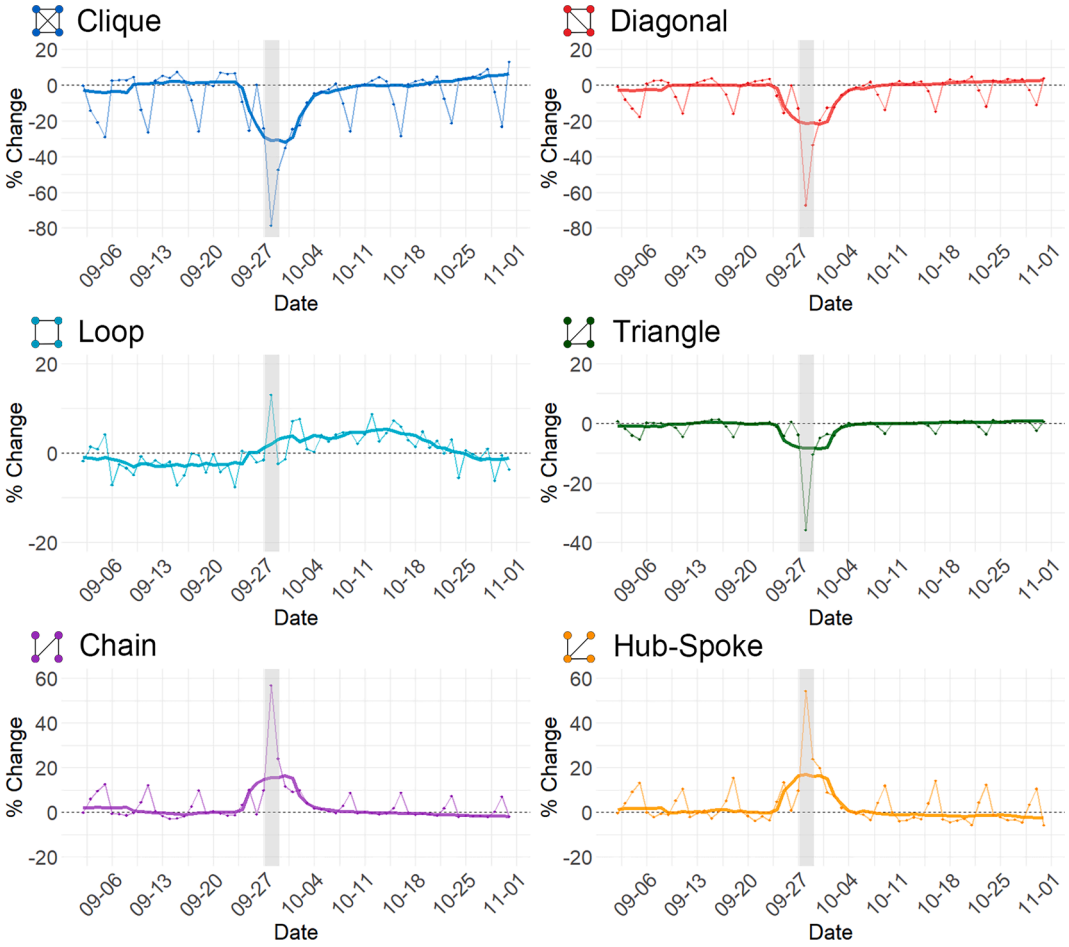

Fig. 6. Percentage change in the distribution of the six motif types during the study period, with the grey bar indicating the period of Hurricane Ian's landfall. Smoothed lines represent the 7-day moving average, while the dashed lines depict the baseline value of each motif type.

Despite having similar average counts throughout the study period, the Chain and Triangle types, as well as the Diagonal and Hub-Spoke types, responded differently to Hurricane Ian's impact. This disparity highlights how external factors like hurricanes can disproportionately affect more connected motifs in mobility networks, penalizing these structures for their complexity and interconnectedness.

Fig. 7 illustrates the average edge weight and average edge distance for the 6 motif types in our mobility network. Notably, substantial variations were observed in the average edge weight among motif types, with more connected motifs like the Clique, Diagonal, and Triangle types showing higher average edge weights. This suggests that these motif types, characterized by a greater number of connections, supported more frequent or intense mobility interactions. Interestingly, although the Loop type also has four edges like the more connected motifs, its average edge weight aligned more closely with the Chain and Hub-Spoke types, which have only three edges. This indicates that the intensity of mobility interactions within a motif may not always be directly proportional to the number of its edges. Despite variations in the average edge weight among motif types, they all showed a similar temporal trend in the average edge weight throughout Hurricane Ian. Among motif types, there was a noticeable decline in the average edge weight during the hurricane's landfall, followed by a gradual return to normal levels over approximately three weeks. The weekly pattern was also clear in the average edge weight across motif types both before and after the landfall, but it was disrupted during the recovery phase. This consistent temporal pattern across motif types suggests a widespread, albeit temporary, disruption in mobility behaviors caused by the hurricane.

In terms of the average edge distance for each motif type, it was observed that the more interconnected motifs tended to have shorter travel distances, indicating more localized or concentrated movements within these complex structures. Before the landfall, the average edge distance for the Clique type remained around 21 km, while it was about 40 km for the Hub-Spoke type. At landfall, their

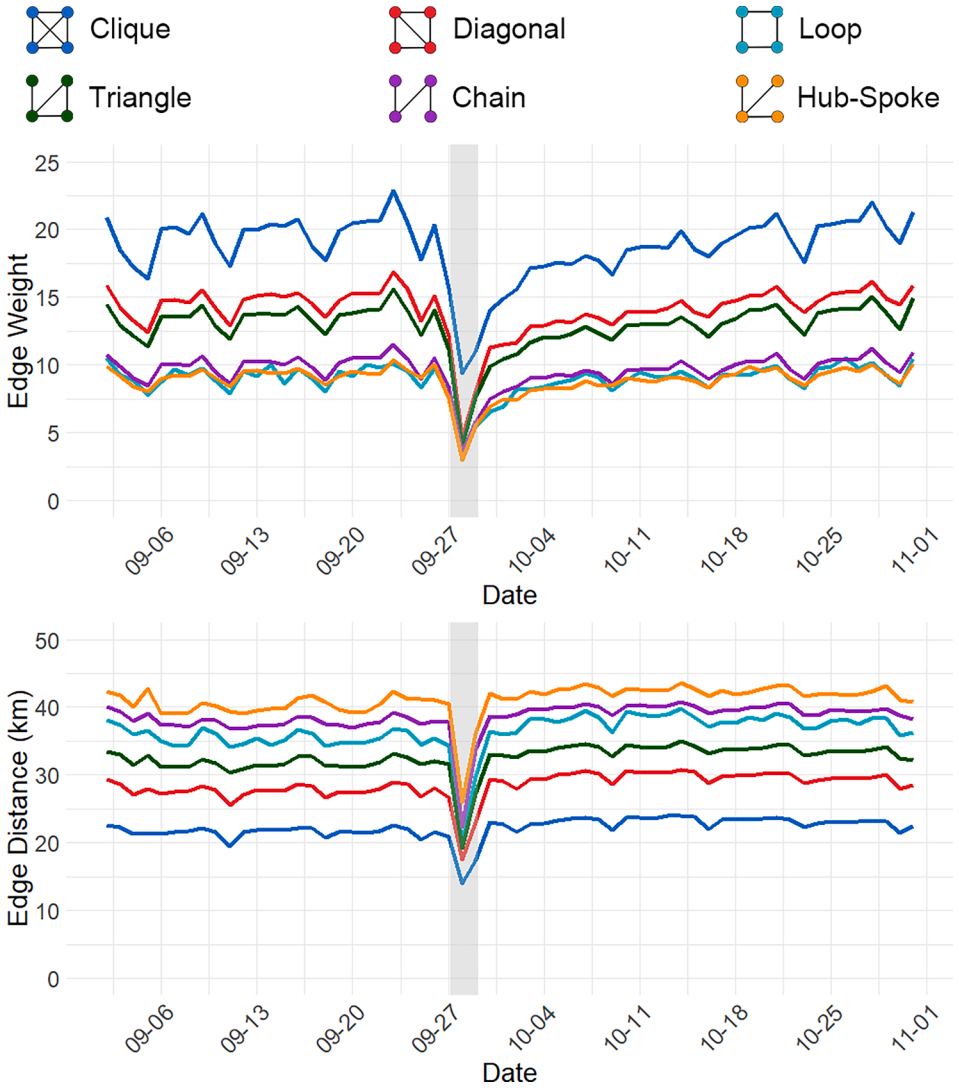

Fig. 7. Average edge weight and edge distance across the six motif types, with the grey bar indicating the period of Hurricane Ian's landfall.

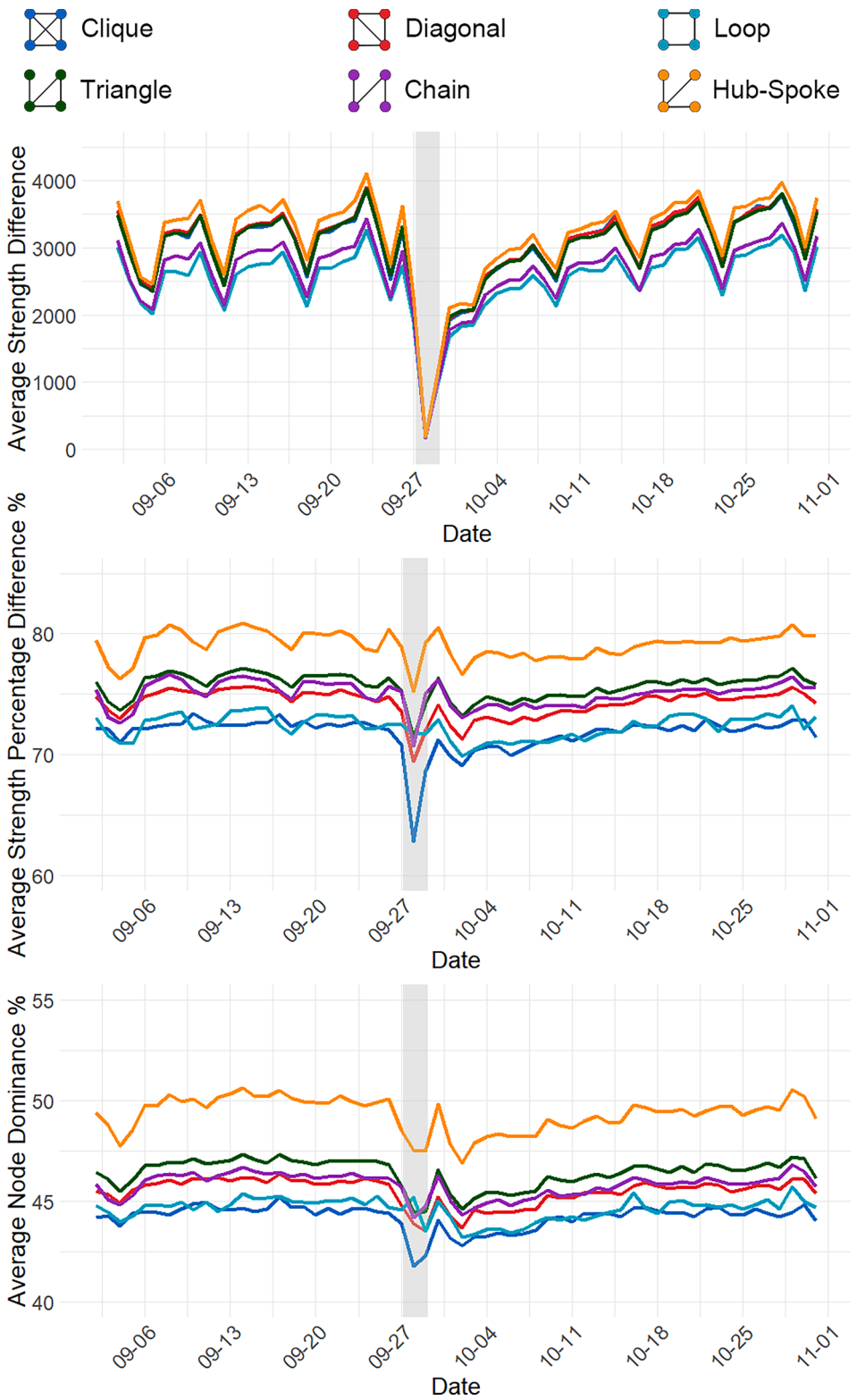

Fig. 8. Results of three node strength metrics across the six motif types, with the grey bar indicating the period of Hurricane Ian's landfall.

average edge distance dropped to 14 km and 25 km, respectively, indicating a 33 % and 37 % reduction. Other motif types exhibited a similar decrease in percentage. Interestingly, the impact of Hurricane Ian on the average edge distance across motif types was relatively short-term compared to its impact on the edge weight. Within just two days, the average edge distance for all motif types returned to normal levels. Weekly trends also emerged for all motif types, with no disruptions observed during the recovery period.

Fig. 8 presents the results on changes in node strength metrics for each motif type, providing insights into individual nodes' contributions to the overall structure and resilience of the mobility network during Hurricane Ian's impact. This analysis includes three metrics. Firstly, the average node strength difference for each motif type is calculated by determining the disparity between the highest and lowest node strengths within motifs of the same type and then averaging these differences. Secondly, the average percentage difference is calculated by dividing this average strength difference by the highest node strength in the motif. Lastly, the average node dominance is calculated by dividing the highest node strength in the motif by the total node strength of that motif.

The Hub-Spoke type showed the highest values across all three metrics, reflecting its distinct structure, often leading to notable differences among nodes within the motif. A consistent trend was observed in the average strength difference among all motif types, mirroring the pattern noted in the average edge weight analysis. This trend indicated a marked decrease in node strength differences during Hurricane Ian's impact, followed by a gradual return to normal levels as well as a clear weekly trend. Conversely, the Chain and Loop types consistently exhibited the lowest discrepancies in node strength throughout the study period, despite the unequal importance of nodes within the Chain type. This suggests a relatively equitable distribution of node strengths within the Chain type, even amidst varying structural conditions.

Regarding the average percentage difference in node strength, most motif types experienced a decline during Hurricane Ian's impact, except for the Loop type, which remained relatively steady. While the decrease in percentage difference was less pronounced

Table 2
The Interquartile Range results of the motif metrics between Sept 27th and Oct 1st.

	9/27/22	9/28/22	9/29/22	9/30/22	10/1/22
Clique Count	FALSE	TRUE	FALSE	FALSE	FALSE
Diagonal Count	FALSE	TRUE	TRUE	FALSE	FALSE
Loop Count	FALSE	TRUE	TRUE	FALSE	FALSE
Triangle Count	FALSE	TRUE	TRUE	FALSE	FALSE
Chain Count	FALSE	TRUE	TRUE	FALSE	FALSE
Hub-Spoke Count	FALSE	TRUE	TRUE	FALSE	FALSE
Clique Percentage	FALSE	TRUE	TRUE	FALSE	FALSE
Diagonal Percentage	FALSE	TRUE	TRUE	FALSE	FALSE
Loop Percentage	FALSE	TRUE	FALSE	FALSE	FALSE
Triangle Percentage	FALSE	TRUE	TRUE	FALSE	FALSE
Chain Percentage	FALSE	TRUE	TRUE	FALSE	FALSE
Hub-Spoke Percentage	FALSE	TRUE	TRUE	TRUE	FALSE
Clique Avg Distance	FALSE	TRUE	TRUE	FALSE	FALSE
Diagonal Avg Distance	FALSE	TRUE	TRUE	FALSE	FALSE
Loop Avg Distance	FALSE	TRUE	TRUE	FALSE	FALSE
Triangle Avg Distance	FALSE	TRUE	TRUE	FALSE	FALSE
Chain Avg Distance	FALSE	TRUE	TRUE	FALSE	FALSE
Hub-Spoke Avg Distance	FALSE	TRUE	TRUE	FALSE	FALSE
Clique Avg Weight	FALSE	TRUE	TRUE	FALSE	FALSE
Diagonal Avg Weight	FALSE	TRUE	TRUE	FALSE	FALSE
Loop Avg Weight	FALSE	TRUE	TRUE	FALSE	FALSE
Triangle Avg Weight	FALSE	TRUE	TRUE	FALSE	FALSE
Chain Avg Weight	FALSE	TRUE	TRUE	FALSE	FALSE
Hub-Spoke Avg Weight	FALSE	TRUE	TRUE	FALSE	FALSE
Clique Absolute Diff	FALSE	TRUE	TRUE	FALSE	FALSE
Diagonal Absolute Diff	FALSE	TRUE	TRUE	FALSE	FALSE
Loop Absolute Diff	FALSE	TRUE	TRUE	FALSE	FALSE
Triangle Absolute Diff	FALSE	TRUE	TRUE	FALSE	FALSE
Chain Absolute Diff	FALSE	TRUE	TRUE	FALSE	FALSE
Hub-Spoke Absolute Diff	FALSE	TRUE	TRUE	FALSE	FALSE
Clique Percentage Diff	FALSE	TRUE	TRUE	FALSE	FALSE
Diagonal Percentage Diff	FALSE	TRUE	FALSE	FALSE	FALSE
Loop Percentage Diff	FALSE	FALSE	FALSE	FALSE	FALSE
Triangle Percentage Diff	FALSE	TRUE	FALSE	FALSE	FALSE
Chain Percentage Diff	FALSE	TRUE	FALSE	FALSE	FALSE
Hub-Spoke Percentage Diff	FALSE	TRUE	FALSE	FALSE	FALSE
Clique Node Dominance	FALSE	TRUE	TRUE	FALSE	TRUE
Diagonal Node Dominance	FALSE	TRUE	TRUE	FALSE	FALSE
Loop Node Dominance	FALSE	FALSE	FALSE	FALSE	FALSE
Triangle Node Dominance	FALSE	TRUE	TRUE	FALSE	FALSE
Chain Node Dominance	FALSE	FALSE	FALSE	FALSE	FALSE
Hub-Spoke Node Dominance	FALSE	FALSE	FALSE	FALSE	FALSE

Note: Any metric value that exceeds 1.5 times the IQR above the third quartile or below the first quartile is classified as an outlier. These outliers are marked as 'TRUE.'.

than the drop in node strength difference, it was still noticeable, suggesting that nodes with higher strength were proportionally more affected than those with lower strength. However, this effect was short-lived, rebounding one day after landfall. Notably, the weekly pattern observed before Ian's impact significantly decreased post-impact, suggesting possible enduring changes in the network's dynamics.

The average node dominance metric demonstrated a brief yet notable impact from Hurricane Ian, with a rapid recovery observed across all motif types. However, an intriguing spike in dominance was noted immediately after landfall, followed by a sharp decline across all motif types. This trend implies that nodes with higher strength in the motif recovered more quickly, initially enhancing average node dominance. Subsequently, as lower-strength nodes began to recover the following day, a marked decrease in average node dominance was observed. These findings collectively enhance our understanding of the dynamic interplay of node strengths within different motif types and their adaptability to external disruptions such as hurricanes.

To determine whether the disruptions in motif metric trends, particularly around the hurricane landfall, were meaningful, the Interquartile Range (IQR) is calculated for each motif type, for each day between September 27th and October 1st. The IQR captures the spread of the middle 50 % of the data, helping to identify outliers and assess if the metric values during the hurricane period (September 27th to October 1st) deviated notably from the rest of the timeframe. Specifically, any metric value that exceeds 1.5 times the IQR above the third quartile or below the first quartile is classified as an outlier. In Table 2, these outliers are marked as 'TRUE.' As presented in Table 2, the results closely align with our initial observations: on September 28th, the day of landfall, most metrics were flagged as outliers, with the exception of a few associated with the Loop motif, which aligns with the patterns seen in the plots. On September 29th, the overall trend persisted, though a few metrics, including percentage differences in certain motifs, were no longer classified as outliers. By September 30th and October 1st, nearly all motif metrics had stabilized and returned to typical levels. It is important to highlight that, despite evacuation orders being issued on September 27th in the region, the day before landfall, none of the motif metrics significantly deviated from the overall distribution (i.e., were flagged as outliers). This suggests that, while some early signs of movement were observable, large-scale evacuations or significant changes in mobility behavior were not yet in full effect. The lack of a noticeable shift in mobility patterns on the 27th could imply either a delayed public response to the evacuation orders or that the majority of residents, with a larger share of older adults, did not immediately act on the orders. This might be due to a variety of factors, such as uncertainty about the storm's severity, reluctance to leave, or logistical challenges in mobilizing within a short timeframe.

4.2.2. Motif spatial distribution patterns

To gain a comprehensive insight into the substructural network dynamics, it's essential to investigate the spatial distribution dynamics across different motif types throughout the hurricane. This involves counting how many times each node (i.e., census tract) appears within each motif type, categorized by the varying significance (or degree) of nodes within the motif. To illustrate, the occurrences of each tract are counted as either a degree-3 node or a degree-1 node in the Hub-Spoke motif. This process enables the visualization of the spatial distribution of nodes with varying importance within a motif, thereby revealing spatial dynamics attributed to the hurricane. Our analysis zooms in on three key dates: one week prior (September 21st), during (September 28th), and one week following (October 5th) the hurricane's landfall. This selection aims to mitigate the influence of routine weekly mobility patterns on our results, thus enabling a more accurate understanding of the hurricane's impact. Similar to the decline in motif counts for each type, a significant decrease was observed in the maximum occurrence frequency for nodes with different degrees in each motif type during the landfall. All maximum occurrence frequencies showed a decrease of over 90 %, with the more connected nodes experiencing even more prominent drops, such as the over 99 % decrease in the maximum occurrence frequency of nodes in the Clique type. One week after the landfall, the spatial distribution of the motifs returned to the state prior to the impact. However, a decrease was noted in the occurrence frequency of coastal tracts west of Fort Myers in all motifs, as this region was the hurricane's landfall location and suffered direct impacts, causing significant damage to transportation infrastructures (Wang et al., 2024).

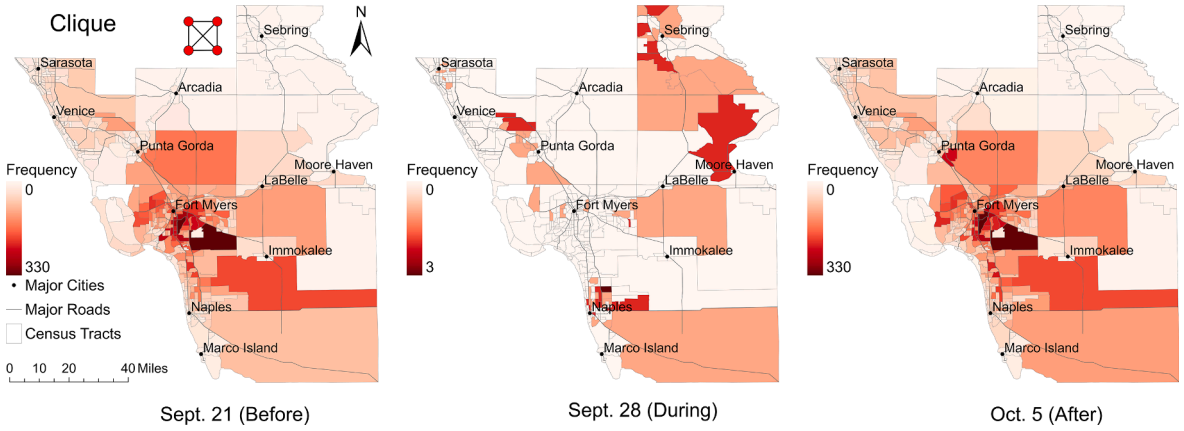

Fig. 9. Frequency of each census tract's occurrence in the Clique motif type before (left), during (middle), and after (right) Hurricane Ian's landfall.

Fig. 9 illustrates the frequency of each census tract's occurrence in the Clique motif type throughout the hurricane. Our observations before and after the hurricane's landfall revealed a notable hotspot of Clique-type motifs near downtown Fort Myers. This clustering indicates robust interconnectivity in and around the downtown area, where fully connected motifs were frequently observed. Moving away from the downtown area, the density of these motifs gradually decreased, signaling a decline in interconnectedness.

However, during the hurricane's impact, there was a significant reduction in the frequency of Clique-type motifs. The near absence of these motifs around downtown Fort Myers underscores the substantial impact of Hurricane Ian on the area. This drastic reduction in interconnected motifs suggests a severe disruption in local movement patterns. In contrast, during the hurricane's landfall, Clique-type motifs clustered near the city of Naples in the southern part of the study area and in the city of Sebring in the northeast. Neither of these areas exhibited clear clustering patterns before or after the hurricane. This distribution suggests that despite the hurricane's widespread disruption, certain areas managed to sustain small-scale yet strongly connected local movements in response to the event. These spatial variations highlight the importance of examining spatial patterns and dynamics within the network structure.

Fig. 10 illustrates the spatial distribution of the frequency of each census tract's appearance in the Diagonal motif type before, during, and after Hurricane Ian's landfall. In contrast to the uniform degree shared by nodes in the Clique motif type, nodes within the Diagonal motif type can possess degrees of either 2 or 3, signifying varying degrees of importance among nodes. Accordingly, occurrences of nodes with different degree values were counted separately. Our analysis revealed a significant difference in the spatial distribution between the two node types within the Diagonal motif type. Before and after Ian's landfall, degree-3 nodes (red census tracts in Fig. 10) were predominantly clustered in a few select census tracts near downtown Fort Myers, suggesting that specific areas near the downtown core exhibited heightened connectivity, with particular tracts serving as hubs within the mobility network. In contrast, the degree-2 nodes distributed more widely across the study area both before and after Ian's landfall, implying a broad and relatively strong level of connectivity across most census tracts. This wider distribution highlights a decentralized network structure, where multiple areas sustain connectivity, albeit with fewer connections compared to the degree-3 nodes.

During Hurricane Ian's landfall, a distinct alteration in the distribution of both node types is noted. Degree-3 nodes clustered prominently in the southern region of the study area, especially within a census tract to the south of the city of Immokalee. This pattern may be attributed to the area being less affected compared to regions around Fort Myers, with the presence of a large inland tract serving as a regional center. Degree-2 nodes also experienced a comparable shift towards the south during Ian's landfall, with the

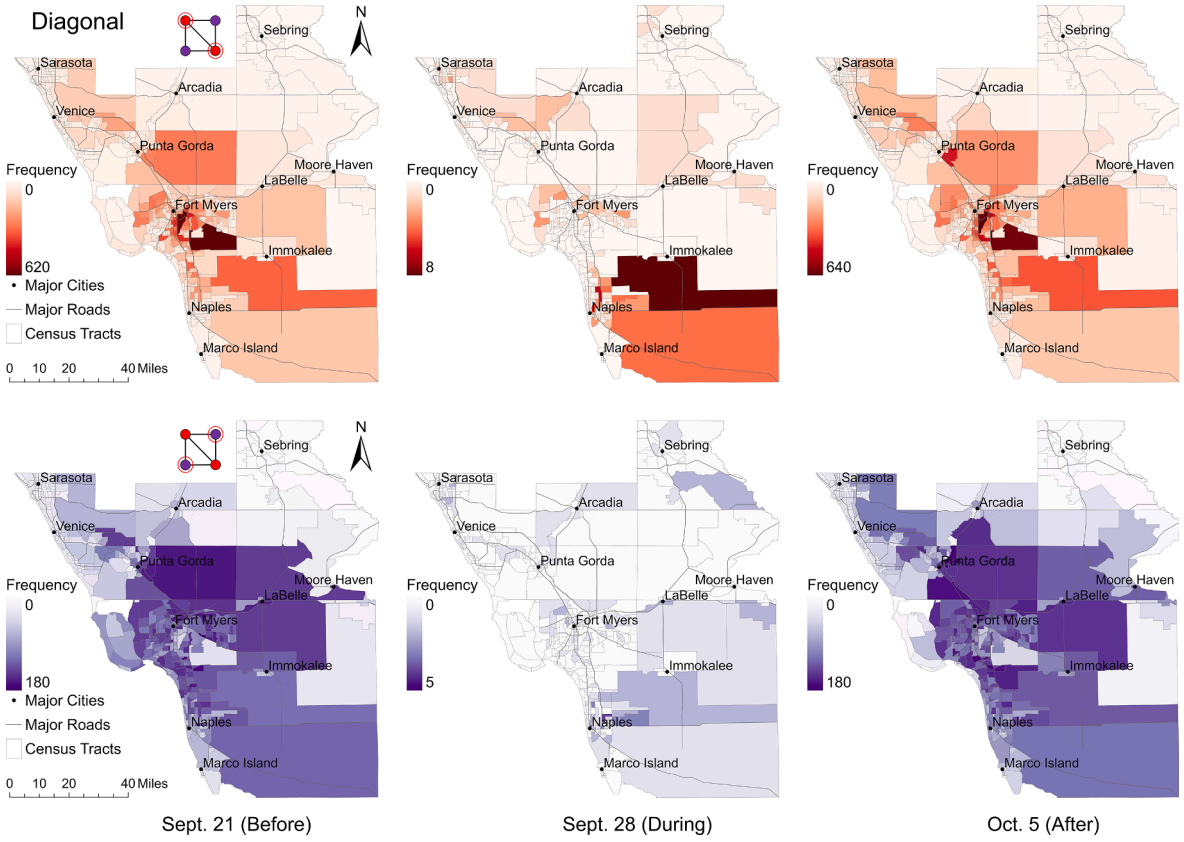

Fig. 10. Frequency of each census tract's occurrence in the Diagonal motif type before (left), during (middle), and after (right) Hurricane Ian's landfall. Degree-3 nodes are colored in red in the top panel, while degree-2 nodes are colored in purple in the bottom panel within this motif type. (For interpretation of the references to color in this figure legend, the reader is referred to the web version of this article.)

hotspots distributed near the city of Naples and Immokalee. Despite the hurricane's impact, the hierarchy of the tracts remained consistent, with the large tract south of Immokalee continuing to serve as a regional mobility center during the landfall.

Characterized by an evenly distributed connection among its four nodes, each of equal importance within the motif, the Loop motif type presents a distinct view of the network's substructure and dynamics. Fig. 11 illustrates the occurrence frequency of each census tract within the Loop motif type before, during, and after Hurricane Ian's impact. Both before and after Ian's landfall, the hotspots of Loop-type motif nodes were spread around Fort Myers, Punta Gorda, Naples, and east of Marco Island. However, no single node dominated in terms of connectivity.

A notable shift occurred in the distribution of nodes within the Loop motif type after Ian's landfall. After the hurricane, this concentration shifted northward, with hotspots appearing near Punta Gorda. The changes observed in the spatial distribution of Loop-type motif nodes before and after the hurricane could suggest shifts in movement patterns and regional focal points due to the hurricane's impact. During the landfall, there were notable changes in the hotspots. Some tracts near Fort Myers, Punta Gorda, and Naples, which were not prominent before and after the landfall, exhibited higher frequencies during the landfall. However, most hotspots before and after Ian's landfall did not display significance during the landfall. This highlights the varying and unpredictable impact of the landfall on tracts within the Loop type motif.

The Triangle motif type stands out as one of the more complex motifs in our analysis. Its complexity stems from the variation in node degrees within the motif: the degree-3 nodes act as hubs, the degree-2 nodes demonstrate relatively strong connectivity, and the degree-1 nodes, while more isolated, link to a well-connected triangle-shaped structure formed by the other higher-degree nodes. Fig. 12 presents the results for the Triangle motif type before, during, and after Hurricane Ian's landfall. For the degree-3 nodes, a consistent pattern of dominance by several census tracts near downtown Fort Myers was observed both before and after Ian's landfall. This suggests that these tracts acted as network hubs sustaining strong connectivity. However, during the hurricane's impact, a notable southward shift occurred in the most frequently appearing degree-3 tracts. This shift mirrors the behavior observed in the degree-3 nodes of the Diagonal motif type, indicating a comparable response to the hurricane's impact across different motif structures.

The degree-2 nodes in the Triangle motif type were dispersed across the central part of the study area. They appeared more frequently around downtown Fort Myers and Punta Gorda both before and after the landfall. Like the degree-3 nodes, these nodes also experienced a southward shift during Ian's landfall, becoming more concentrated near Naples and Immokalee. Nonetheless, certain degree-2 nodes remained near Fort Myers during the landfall, suggesting that the Triangle motif type may be more resilient within the mobility network compared to the Diagonal type, even amid disruptive events.

As for the degree-1 nodes, the results aligned with expectations. Both before and after the hurricane, the hotspots of degree-1 nodes were situated farther from downtown Fort Myers. Instead, census tracts near smaller cities like Arcadia, Immokalee, LaBelle, and Moore Haven emerged as hotspots. This distribution indicates that while these nodes are part of a connected motif, they typically lie on the periphery of the network's core areas. During Ian's landfall, the hotspots of degree-1 nodes remained positioned away from downtown Fort Myers but were relatively closer, consistent with the observed reduction in motif travel distance during the hurricane. This suggests that while peripheral areas maintained their connectivity, the overall mobility network contracted, resulting in nodes closer to central areas becoming isolated.

The Chain motif type, which resembles a linear arrangement, features two nodes at each end with a degree of 1, along with two intermediate nodes that serve as transitional points. While these intermediate nodes play a crucial role in the motif, they do not possess the strong connectivity of hubs, nor are they as isolated as degree-1 nodes, maintaining a balanced position within the structure. This characteristic makes the Chain motifs susceptible to transitioning into other motif types under certain conditions. Fig. 13 illustrates the results for the Chain motif type before, during, and after Hurricane Ian's landfall. Our findings indicate that the hotspots of degree-2 nodes in the Chain type were situated near Punta Gorda in the northern part of the study area, both before and after Hurricane Ian's landfall. This distribution suggests that tracts in these areas typically demonstrate good connectivity and serve as the local transitioning centers but lack the level of interconnection required to be considered highly integrated within the network. The presence of

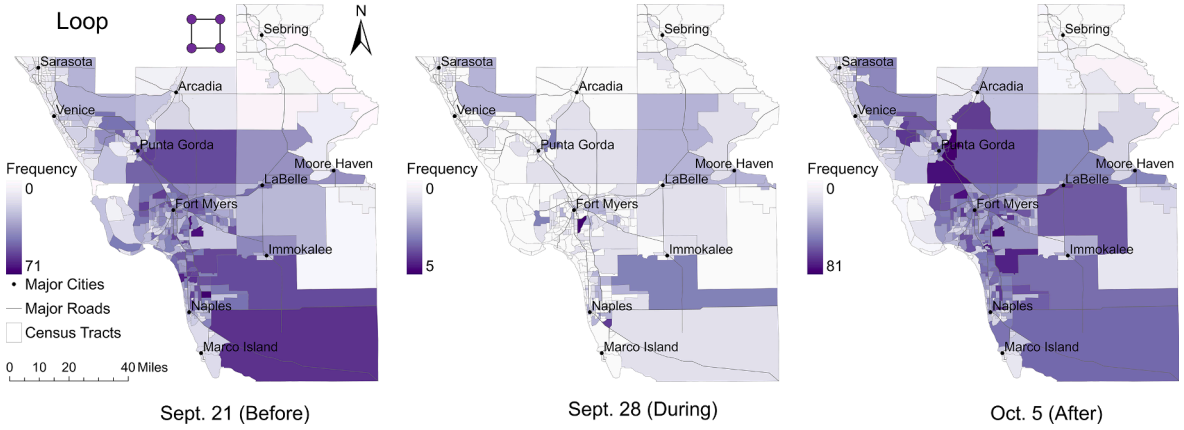

Fig. 11. Frequency of each census tract's occurrence in the Loop motif type before (left), during (middle), and after (right) Hurricane Ian's landfall.

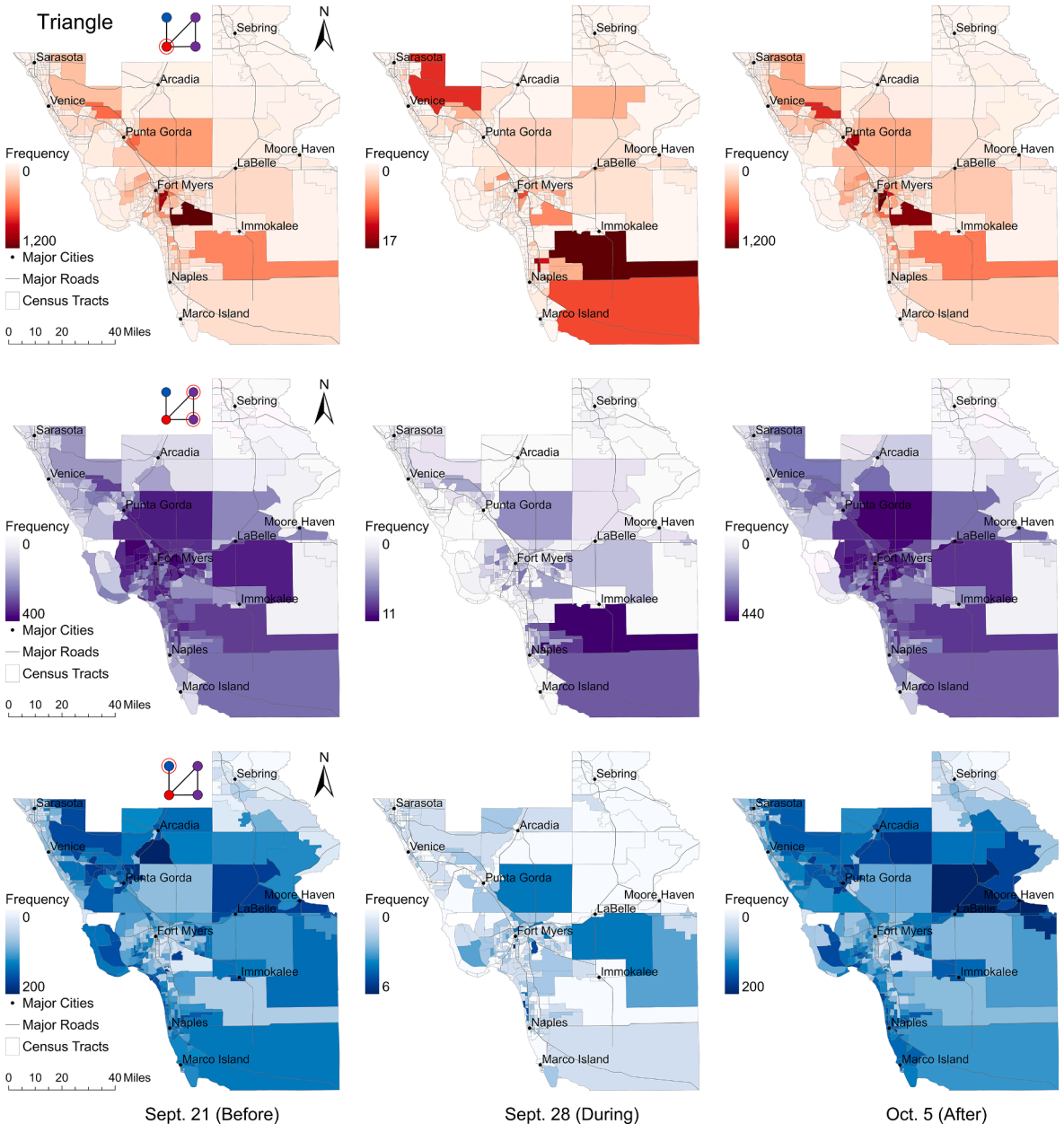

Fig. 12. Frequency of each census tract's occurrence in the Triangle motif type before (left), during (middle), and after (right) Hurricane Ian's landfall. Degree-3 nodes within this motif type are colored in red in the top panel, while degree-2 nodes are colored in purple in the middle panel and degree-1 nodes are colored in blue in the bottom panel. (For interpretation of the references to color in this figure legend, the reader is referred to the web version of this article.)

these nodes in the Chain motif type highlights a level of connectivity that facilitates linear movement patterns without centralizing around a specific hub. During the hurricane's impact, there was a noticeable southward migration observed in the hotspots for the degree-2 nodes. This shift led to two tracts in the southern part showing a higher frequency of representation within the Chain motif type. This suggests that these tracts assumed a heightened role as transitional centers during the hurricane's landfall, possibly influenced by evacuation patterns.

The degree-1 nodes were widely dispersed across the study area both before and after Ian's landfall. Interestingly, coastal tracts, including those near Sarasota and Venice, appeared more frequently in the Chain motif type as the degree-1 nodes compared to other motif types. This pattern might be attributed to the unique structure of the Chain motif type and the geographic constraints of coastal tracts. Occupying the end a chain motif requires less connectivity than being part of more interconnected motifs, thus making these locations more likely to appear as degree-1 nodes in the Chain type. During Hurricane Ian's landfall, a contraction in the spatial

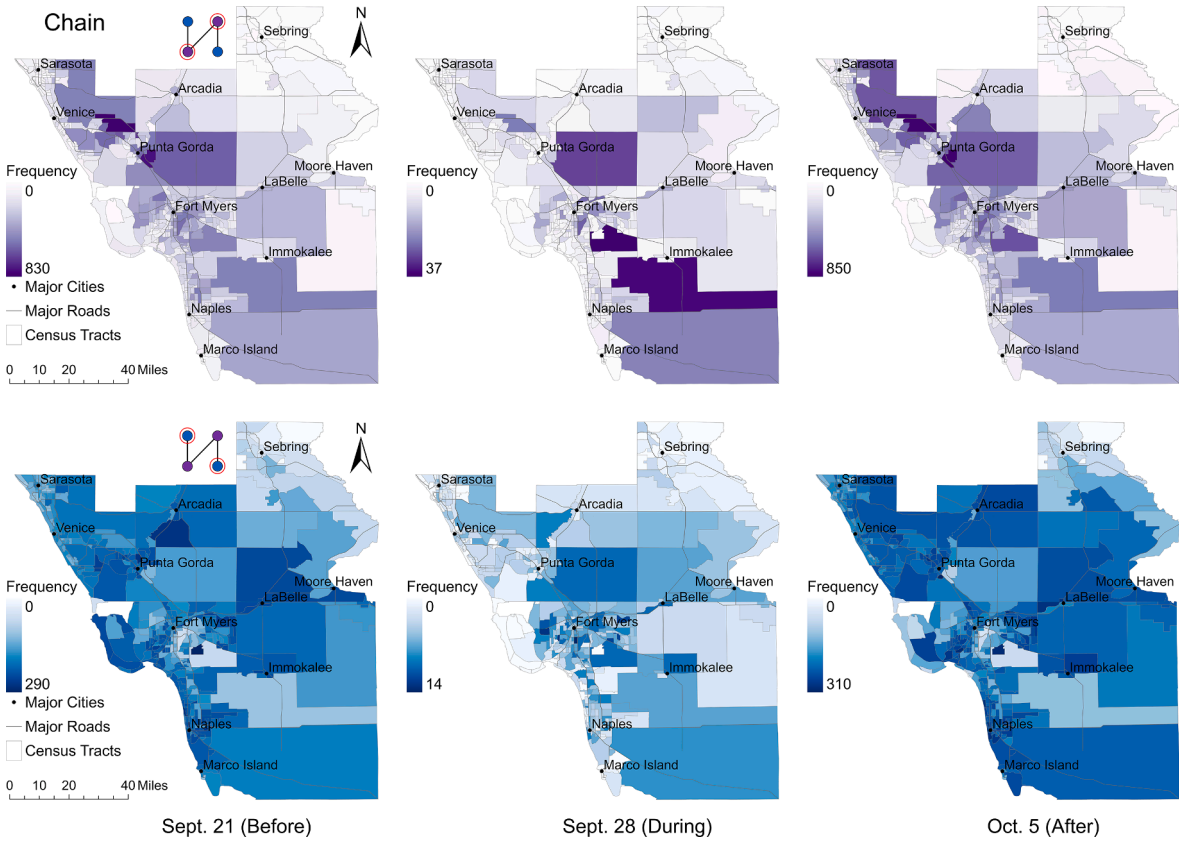

Fig. 13. Frequency of each census tract's occurrence in the Chain motif type before (left), during (middle), and after (right) Hurricane Ian's landfall. Degree-2 nodes within this motif type are colored in purple in the top panel, while degree-1 nodes are colored in blue in the bottom panel. (For interpretation of the references to color in this figure legend, the reader is referred to the web version of this article.)

distribution of degree-1 nodes was observed, similar to the observations in the Triangle motif type. Hotspots for degree-1 tracts were situated nearer to the downtown area of Fort Myers, Punta Gorda, and Naples, indicating a decrease in the overall motif distance. This contraction suggests a compression of the mobility network at the substructure level during the hurricane's impact, resulting in more localized and less extensive movements.

The Hub-Spoke motif type presents a distinct substructure within the mobility network, characterized by a notable contrast in node roles. In this motif, the degree-3 node functions as a central hub, linking to all other three nodes, which are relatively isolated. These three nodes have the potential to transform the Hub-Spoke motif into another type if further connections are established among them. Fig. 14 shows the results for the Hub-Spoke motif type before, during, and after Hurricane Ian's landfall. Both before and after the hurricane, certain tracts consistently stood out as prominent hotspots for the degree-3 hub node. These include two tracts near downtown Fort Myers, which also assumed similar roles in other motif types. However, the Hub-Spoke type also revealed two tracts near Punta Gorda in the north as an additional hotspot for the degree-3 nodes. These tracts, which were less prominent in the Clique and Diagonal motif types, suggest strong local connections primarily to nearby isolated tracts rather than the broader network. During the hurricane's landfall, there was a noticeable shift in the hotspots of degree-3 hub nodes towards the south, indicating the persistence of local connectivity in that area. This shift demonstrates a reorientation of the hub nodes in response to the hurricane, preserving their central role in their nearby surroundings. Meanwhile, one of the hotspot nodes near Punta Gorda retained its status as a local hub in the northern region during the landfall.

The degree-1 spoke nodes were widely dispersed across the study area both before and after the hurricane's landfall with a cold spot near downtown Fort Myers. During the landfall, a contraction pattern similar to that observed in degree-1 nodes in other motif types was observed, with hotspots clustering nearer to the downtown areas of major cities like Fort Myers and Naples. Despite these changes, the majority of nodes in this motif remained connected to local hubs, underscoring a resilient aspect of this particular network substructure.

5. Discussion and conclusions

This research investigates the impact of Hurricane Ian on human mobility patterns and the subsequent recovery in southwest Florida. Using privacy-preserving GPS data from mobile phones, the study constructs human mobility networks before, during, and

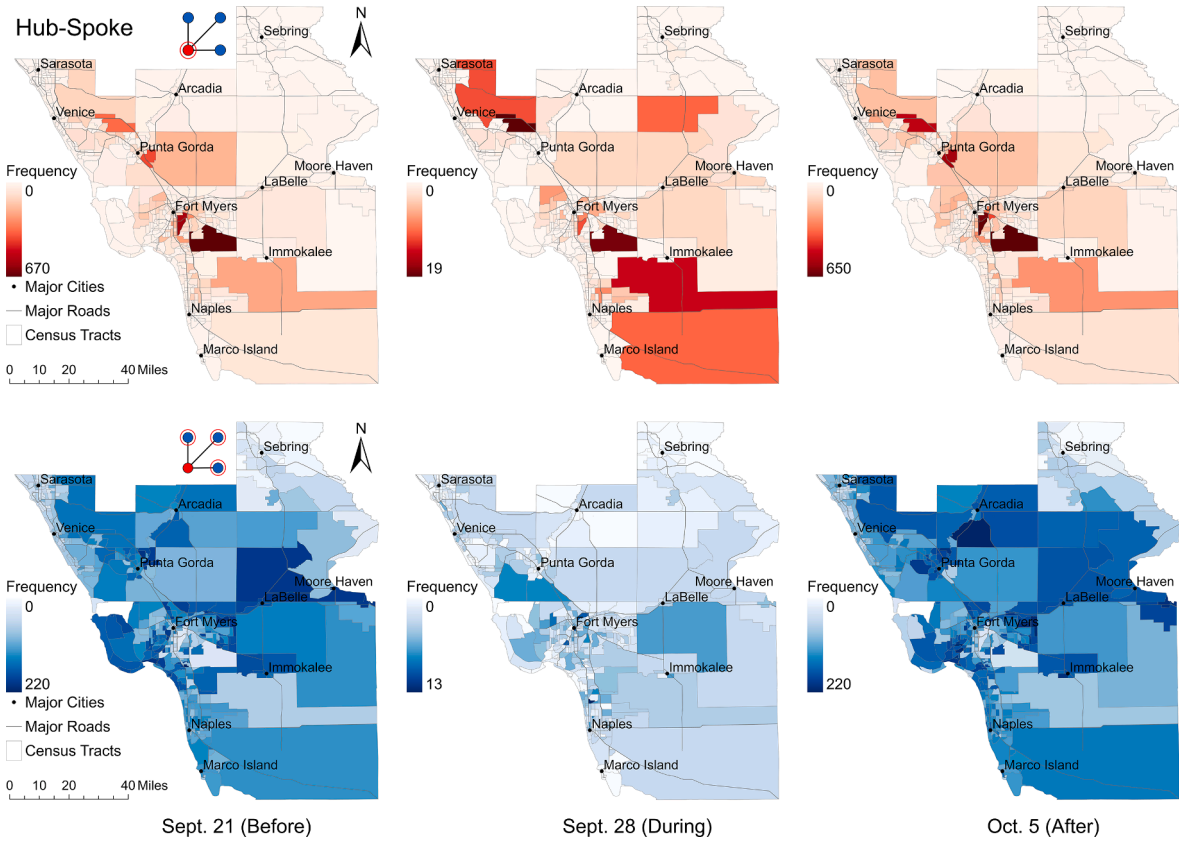

Fig. 14. Frequency of each census tract's occurrence in the Hub-Spoke motif type before (left), during (middle), and after (right) Hurricane Ian's landfall. Degree-3 nodes within this motif type are colored in red in the top panel, while degree-1 nodes are colored in blue in the bottom panel. (For interpretation of the references to color in this figure legend, the reader is referred to the web version of this article.)

after the hurricane. Structural characteristics of these networks are analyzed at both macro and substructure (motif) levels. This multiscale approach is adopted because measures at a singular scale may not fully capture the effects and recovery patterns within the network. Additionally, this research examines spatial variations in motifs over time, offering insights into spatialized connectivity patterns and their adaptations in response to the hurricane's impact.

During the hurricane's impact, the macroscale analysis of human mobility networks demonstrates significant shifts in mobility patterns. The immediate consequence was a notable reduction in mobility, as evidenced by the total edge weight dropping by nearly 90 %, and network density decreasing by about 80 %, indicating a marked reduction in overall connectivity. Local connectivity and network efficiency were also disrupted, demonstrated by a 40 % decline in the average clustering coefficient and a 55 % increase in the average path length, indicating a substantial reduction in connections and the network's efficiency. The modularity increased by 140 %, while reciprocity decreased by 15 %, suggesting a transition towards more localized mobility patterns and unidirectional flows, likely influenced by evacuation orders and safety precautions.

The recovery phase highlights the resilience and adaptability of the human mobility network. Notably, the total edge weight and network density demonstrated resilience by swiftly recovering and surpassing baseline levels within two weeks and one week, respectively, after the hurricane. Similarly, the network's robustness measures rebounded fully within just 2–3 days after a slight decline on the day of landfall, underscoring the network's structural resilience and its capability to sustain connectivity even under significant disruptions. The average path length also quickly returned to baseline levels within about five days, again indicating the swift restoration of network efficiency and connectivity. However, despite the resilience, some metrics pointed to enduring changes in the network's structure following Hurricane Ian's impact. The average clustering coefficient did not revert to its pre-impact levels, signaling enduring changes in local connectivity patterns. Modularity remained slightly lower than the baseline post-recovery, suggesting a trend towards less cohesive community structures. Moreover, reciprocity did not fully recover, indicating sustained changes in mobility dynamics, potentially leading to the emergence of more unidirectional movement patterns. These enduring changes highlight the complex interplay between resilience and long-term impacts, underscoring the importance of understanding these dynamics to improve disaster response and preparedness strategies.

At the substructural scale, the mobility networks' response to Hurricane Ian reveals a pattern characterized by disruption, resilience, and potential adaptation. Each motif type experienced a significant decrease in count during the impact, followed by a gradual recovery spanning approximately one week. The hurricane's landfall notably impacted the motif percentage distribution, particularly

in highly interconnected motifs such as Clique and Diagonal types, which experienced considerable reductions. This highlights the vulnerability of densely connected mobility substructures to external disruptions. Conversely, motifs with lower connectivity, such as the Chain and Hub-Spoke types, showed an increase in their percentage distribution among all motifs, possibly suggesting heightened evacuation and gathering activities during the hurricane. The Loop type showed a gradual rise in its percentage distribution among all motifs and returned to normal about a month later. Aside from the Loop type, the counts of other motif types returned to pre-hurricane conditions within a week. This varied recovery rate highlights different levels of resilience and adaptability across network substructures, with some areas possibly requiring longer to recover due to more extensive damage or slower restoration efforts.

There was also a reduction in the average edge weight and distance across all motif types, suggesting decreased mobility volume and distance during the hurricane. While the average edge weight exhibited a gradual recovery over two weeks, edge distance rebounded within just 2–3 days, possibly reflecting the quick reinstatement of essential short-distance connections critical for immediate post-disaster responses and recovery activities. Interestingly, motifs with stronger connections (i.e., Clique type) tended to encompass tracts in shorter distance to each other, a pattern that persisted during the impact. Furthermore, node strength metrics in most motifs decreased during the hurricane, except for the Loop type, indicating that it may have maintained or even enhanced its functional role during the hurricane, possibly supporting continuous local movements and connectivity in specific areas. Although the average strength difference for all types gradually recovered, there was a spike in the strength percentage difference and node dominance two days after the landfall, followed by a gradual recovery. This suggests that nodes with greater strength within motifs experienced faster recovery compared to others. Additionally, motifs with distinct internal hierarchies, like the Hub-Spoke type, displayed higher strength percentage difference and node dominance. This demonstrates their central role in the recovery phase, possibly functioning as main arteries in the reconstitution of the network and emergency services distribution.

The spatial distribution visualization of motifs across census tracts (nodes) in this study offers insights into the dynamics of human mobility networks, particularly in response to Hurricane Ian. Each motif type – Clique, Diagonal, Loop, Triangle, Chain, and Hub-Spoke – revealed unique patterns and variations in node appearances, underscoring the diverse connectivity and resilience present within the network. However, the coastal tracts west of Fort Myers are the major areas showing significant changes post-impact across all motifs, attributable to the hurricane's direct landfall and infrastructure damage. Both before and after the hurricane, the concentrated presence of Clique and Diagonal motifs near downtown Fort Myers indicates its significance as a hub for intense interconnectivity, facilitating crucial movement within the network. However, the hurricane's onset resulted in a noticeable reduction in the occurrence of these motifs near downtown Fort Myers, shifting their presence southward, particularly near Naples. Conversely, prior to the hurricane, the Loop type exhibited lower concentration compared to the Clique and Diagonal type, with hotspots widely scattered in the western and southern parts of the study area. During the landfall, only a few hotspots remained near Fort Myers, Naples, and Punta Gorda, which were not noticeable before the event. After the landfall, the hotspots near Naple showed a decrease in occurrence frequency, while the ones near Punta Gorda appeared to increase in frequency. This also happens in one tract near Punta Gorda, which could indicate a stronger recovery in that region.

Within the Triangle motif type, both the degree-3 and degree-2 nodes exhibited a comparable southward shift like the Clique and Diagonal types, converging toward the Naples region during the landfall. Meanwhile, the degree-1 nodes, being the most isolated nodes within the motif, were spread farther from Fort Myer. Nonetheless, a contraction of degree-1 node hotspots was observed in tracts nearer to the Fort Myers, coinciding with the reduced average edge distance. In the Chain motif type, the degree-2 node hotspots were located near the city of Punta Gorda both before and after the landfall. However, during the landfall, these hotspots shifted to large tracts near Fort Myers and Immokalee, indicated a change in the transition tract locations, possibly due to evacuation behaviors. Additionally, more coastal tracts appeared as the degree-1 nodes in the Chain type. Despite the degree-1 nodes being distributed away from Fort Myers, a similar contraction was observed during the landfall. The Hub-Spoke motif within the mobility network highlights a notable distinction in node functions, where degree-3 nodes act as central hubs linked to more isolated nodes, which were predominantly clustered around a few tracts near Fort Myers. During the landfall, these hotspots relocated to a few tracts in the south, including areas near Naples. Meanwhile, degree-1 "spoke" nodes displayed a broad distribution before the hurricane, which then condensed during the hurricane, concentrating near urban centers, suggesting a network-wide contraction.

The multiscale analysis in this study, including dynamics in structural properties at both macro and substructure levels, as well as dynamics in the spatial distribution of network substructures (motifs), offers insights to enhance policymaking in disaster management and urban planning. By examining the human mobility network's response to Hurricane Ian across different scales, this study aids in identifying areas of resilience and vulnerability, which is crucial for developing targeted and effective disaster response strategies. At the macroscale, the examination of the mobility network's overall structure and connectivity reveals the broad impacts of the hurricane on patterns of human movement and infrastructure utilization. This level of analysis can guide policymakers in enhancing the resilience of critical transportation networks and urban infrastructure. For example, the rapid recovery of specific network metrics following the hurricane suggests that certain edges and nodes are inherently more resilient. Strengthening these critical components could ensure that key routes remain operational, facilitating efficient emergency responses and swift recovery.

Our in-depth motif analysis reveals distinct resilience patterns within the mobility network, offering valuable insights for optimizing disaster response strategies. For instance, recognizing which motifs—specific patterns of connectivity—remain resilient or quickly recover enables emergency planners to pinpoint potential hubs of activity and connectivity that are crucial during a disaster. Notably, motifs like Chains and Hub-Spokes became more prominent during Hurricane Ian, indicating their crucial role in evacuation and emergency coordination efforts. Moreover, these motifs also demonstrated inherent structural resilience. To leverage these findings, emergency planners should strategically place permanent emergency shelters, medical units, and supply distribution centers in areas where these motifs like Chains and Hub-Spokes are prevalent, particularly in urban centers such as Fort Myers and Naples. Strengthening the infrastructural in these areas—by reinforcing buildings and ensuring reliable power and water supplies—will ensure

these hubs remain fully operational during disasters. Furthermore, integrating smart technology systems for real-time response and communication can greatly enhance the efficiency of these hubs in disaster situations.

The spatial analysis of network motifs within the mobility network provides valuable insights into the spatial dynamics of mobility patterns during the hurricane. Overall, it highlights significant southward shifts in mobility and substantial impacts on the western coastal areas near Fort Myers. To mitigate these vulnerabilities, targeted infrastructure resilience strategies are crucial. Specifically, enhancing urban resilience in central Fort Myers should be a priority, focusing on strengthening infrastructure in downtown areas that showed robust connectivity before the hurricane. This involves upgrading building codes, improving utility systems, and investing in flood-resistant construction. Moreover, Fort Myers should be prioritized for disaster recovery simulations and emergency response training. It's important to establish secondary emergency operation centers in Naples and Immokalee, as these locations demonstrated strategic value during Hurricane Ian. Ensure these centers are well-stocked with emergency supplies, communication tools, and medical resources. It is advised to strengthen transportation and public infrastructure to better meet increased demands during emergencies, and to install advanced coastal defense systems like elevated barriers and reinforced seawalls, especially in coastal regions west of Fort Myers. Additionally, improving evacuation protocols in southern regions around Naples and Immokalee is crucial. Leveraging Punta Gorda's stable connectivity can also enhance local emergency services and infrastructure resilience. Furthermore, expanding community disaster preparedness programs and establishing local volunteer response teams will contribute to more effective disaster management.

This research has several limitations. One of the primary limitations is the reliance on mobile phone GPS tracking data sourced from Cuebiq. While this data is valuable, it is not exhaustive and may not represent the entire population affected by Hurricane Ian. Certain demographics, such as older adults or those without smartphones, might be underrepresented in the data. This limitation could affect the generalizability of our findings to the entire population impacted by the hurricane. Furthermore, this study does not incorporate socio-economic characteristics into the analysis, which may hinder our understanding of community-specific impacts and recoveries. Integrating such data could offer a more comprehensive understanding of disaster responses, facilitating the development of targeted and effective recovery strategies. Another limitation is the focus on a specific geographic area (Southwest Florida) and a single event (Hurricane Ian). While this allowed for a detailed analysis of this particular scenario, it may limit the applicability of our findings to other regions or different types of natural disasters. Different areas and disaster contexts might exhibit unique mobility patterns and network responses. Nonetheless, the proposed methods can be readily adapted for use in other regions or disaster events where data is available. Lastly, the study does not account for potential changes in the physical environment due to the hurricane, such as road closures or infrastructure damage, which could have a significant impact on mobility patterns.

CRediT authorship contribution statement

Jinpeng Wang: Writing – original draft, Visualization, Methodology, Formal analysis. **Yujie Hu:** Writing – review & editing, Writing – original draft, Supervision, Project administration, Methodology, Funding acquisition, Conceptualization.

Declaration of competing interest

The authors declare that they have no known competing financial interests or personal relationships that could have appeared to influence the work reported in this paper.

Acknowledgements

The authors thank the editor and the anonymous referees for their valuable comments that greatly improved this article. The authors gratefully acknowledge funding from the U.S. National Science Foundation under Grant #2319551.

Data availability

Data will be made available on request.

References

Ahmouda, A., Hochmair, H.H., Cvetojevic, S., 2019. Using twitter to analyze the effect of hurricanes on human mobility patterns. Urban Sci. 3 (3), 87.

Anderson, C. (2022). *Ian swamps southwest Florida, trapping people in homes*. AP NEWS. https://apnews.com/article/hurricane-ian-live-updates-6302894797cae989ff855030cf332a97.

Anderson, C. (2023). *NOAA: Ian was Cat 5 before weakening at Florida landfall*. AP News. https://apnews.com/article/hurricane-ian-noaa-storm-report-florida-8f2842fc12fd7d06503815307de59c57.

Anguelova, Z., Stow, D.A., Kaiser, J., Dennison, P.E., Cova, T.J., 2010. Integrating Fire Behavior and Pedestrian Mobility Models to Assess Potential Risk to Humans from Wildfires Within the U.S.–Mexico Border Zone*. Prof. Geogr. 62 (2), 230–247.

Barbosa, H., Barthelemy, M., Ghoshal, G., James, C.R., Lenormand, M., Louail, T., Menezes, R., Ramasco, J.J., Simini, F., Tomasini, M., 2018. Human mobility: Models and applications. Phys. Rep. 734, 1–74.

Barnes, M.D., Hanson, C.L., Novilla, L.M.B., Meacham, A.T., McIntyre, E., Erickson, B.C., 2008. Analysis of Media Agenda Setting During and After Hurricane Katrina: Implications for Emergency Preparedness, Disaster Response, and Disaster Policy. Am. J. Public Health 98 (4), 604–610.

Baum, N.L., Rotter, B., Reidler, E., Brom, D., 2009. Building Resilience in Schools in the Wake of Hurricane Katrina. J. Child Adolesc. Trauma 2 (1), 62–70.

Bhattacharya, S., Sinha, S., Dey, P., Saha, A., Chowdhury, C., & Roy, S. (2023, January 1). *Chapter 5 - Online social-network sensing models* (D. Das, A. K. Kolya, A. Basu, & S. Sarkar, Eds.). ScienceDirect; Academic Press.

Binder, S.B., Baker, C.K., Barile, J.P., 2015. Rebuild or Relocate? Resilience and Postdisaster Decision-Making After Hurricane Sandy. Am. J. Community Psychol. 56 (1–2), 180–196.
Bowser, G.C., Cutter, S.L., 2015. Stay or go? Examining decision making and behavior in hurricane evacuations. Environ. Sci. Policy Sustain. Dev. 57 (6), 28–41.
Brevard, S.B., Weintraub, S.L., Aiken, J.B., Halton, E.B., Duchesne, J.C., McSwain, N.E., Hunt, J.P., Marr, A.B., 2008. Analysis of Disaster Response Plans and the Aftermath of Hurricane Katrina: Lessons Learned From a Level I Trauma Center. Journal of Trauma: Injury, Infection & Critical Care 65 (5), 1126–1132.
Burton, C.G., 2014. A Validation of Metrics for Community Resilience to Natural Hazards and Disasters Using the Recovery from Hurricane Katrina as a Case Study. Ann. Assoc. Am. Geogr. 105 (1), 67–86.
Callaway, D.S., Newman, M.E.J., Strogatz, S.H., Watts, D.J., 2000. Network Robustness and Fragility: Percolation on Random Graphs. Phys. Rev. Lett. 85 (25), 5468–5471.
Cao, J., Li, Q., Tu, W., Gao, Q., Cao, R., Zhong, C., 2021. Resolving urban mobility networks from individual travel graphs using massive-scale mobile phone tracking data. Cities 110, 103077.
Chen, Z., Gong, Z., Yang, S., Ma, Q., Kan, C., 2020. Impact of extreme weather events on urban human flow: A perspective from location-based service data. Comput. Environm. Urban Syst. 83, 101520.
Chen, C., Ma, J., Susilo, Y., Liu, Y., Wang, M., 2016. The promises of big data and small data for travel behavior (aka human mobility) analysis. Transport. Res. Part C: Emerg. Technol. 68, 285–299.
Choi, J., Deshmukh, A., Hastak, M., 2016. Increase in stress on infrastructure facilities due to natural disasters. Int. J. Urban Sci. 20 (sup1), 77–89.
Clauset, A., Newman, M.E.J., Moore, C., 2004. Finding community structure in very large networks. Phys. Rev. E 70 (6).
Deng, H., Aldrich, D.P., Danziger, M.M., Gao, J., Phillips, N.E., Cornelius, S.P., Wang, Q.R., 2021. High-resolution human mobility data reveal race and wealth disparities in disaster evacuation patterns. Human. Soc. Sci. Commun. 8 (1).
Fang, J., Hu, J., Shi, X., Zhao, L., 2019. Assessing disaster impacts and response using social media data in China: A case study of 2016 Wuhan rainstorm. Int. J. Disaster Risk Reduct. 34, 275–282.
Fraser, T., 2022. Fleeing the unsustainable city: soft policy and the dual effect of social capital in hurricane evacuation. Sustain. Sci. 17.
Garlaschelli, D., Loffredo, M.I., 2004. Patterns of Link Reciprocity in Directed Networks. Phys. Rev. Lett. 93 (26).
Gomez-Licon, A., 2022. Many trapped in Florida as Ian heads toward South Carolina. WHYY. https://whyy.org/articles/hurricane-ian-tropical-storm-florida-people-trapped-power-outages/.
Gong, Z., Deng, Z., Tang, J., Zhao, H., Liu, Z., Zhao, P., 2024. Uncovering human behavioral heterogeneity in urban mobility under the impacts of disruptive weather events. Int. J. Geogr. Inf. Sci. 1–24.
González, M.C., Hidalgo, C.A., Barabási, A.-L., 2008. Understanding individual human mobility patterns. Nature 453 (7196), 779–782.
Grant, T., 2022. Timeline: When did officials tell people to evacuate from Hurricane Ian? ABC News. https://abcnews.go.com/US/officials-people-evacuate-hurricane-ian/story?id=90931063.
Gunderson, L., 2010. Ecological and Human Community Resilience in Response to Natural Disasters. Ecol. Soc. 15 (2).
Han, S.Y., Tsou, M.-H., Knaap, E., Rey, S., Cao, G., 2019. How Do Cities Flow in an Emergency? Tracing Human Mobility Patterns during a Natural Disaster with Big Data and Geospatial Data Science. Urban Sci. 3 (2), 51.
He, Z., Hu, Y., Duan, L.L., Michailidis, G., 2024. Returners and explorers dichotomy in the face of natural hazards. Sci. Rep. 14 (1).
Hsu, C., Ho, M.A., Mostafavi, A., 2023. Human Mobility Networks Manifest Dissimilar Resilience Characteristics at Macroscopic, Substructure, and Microscopic Scales. Sci Rep 13 (17327).
Ilbeigi, M., & Mostafa Ebrahimi Meimand. (2020). Empirical Analysis of Impacts of Post-Disaster Human Mobility Patterns on the Resilience of Transportation Networks. *Construction Research Congress 2020*.
Jia, S., Kim, S.H., Nghiem, S.V., Doherty, P., Kafatos, M.C., 2020. Patterns of population displacement during mega-fires in California detected using Facebook Disaster Maps. Environ. Res. Lett. 15 (7), 074029.
Jiang, S., Lin, Y., 2022. Ridership and Human Mobility of Metro System Under the Typhoon Weather Event: A Case Study in Fuzhou. China, Urban Rail Transit, p. 8.
Jing, Y., Hu, Y., 2024. Multiscale Complex Network Analysis of Commuting Efficiency: Urban Connectivity, Hierarchy, and Labor Market. Ann. Am. Assoc. Geogr. 1–12.
Kates, R.W., Colten, C.E., Laska, S., Leatherman, S.P., 2006. Reconstruction of New Orleans after Hurricane Katrina: A Research Perspective. Proc. Natl. Acad. Sci. 103 (40), 14653–14660.
Lee, C.-C., Namburi, S., Xiao, X., Mostafavi, A., 2022. Homophilic and Heterophilic Characteristics Shaping Community Formation in Human Mobility Networks During Extreme Weather Response. ArXiv.org.
Li, X., Qiang, Y., Cervone, G., 2024. Using human mobility data to detect evacuation patterns in hurricane Ian. Ann. GIS 1–19.
Maas, P., Almquist, Z., Giraudy, E., & Schneider, J. W. (2020). Using social media to measure demographic responses to natural disaster: Insights from a large-scale Facebook survey following the 2019 Australia Bushfires. *ArXiv:2008.03665 [Cs, Stat]*.
Marinescu, D.C., 2017. Managing Complexity of Large-Scale Cyber-Physical Systems. Elsevier EBooks 65–112.
Mayer, B.W., Moss, J., Dale, K., 2008. Disaster and Preparedness: Lessons from Hurricane Rita. J. Conting. Crisis Manag. 16 (1), 14–23.
Mazzei, P., Bogel-Burroughs, N., Robles, F., Healy, J., 2022. Hurricane Ian's Staggering Scale of Wreckage Becomes Clear in Florida. The New York times. https://www.nytimes.com/2022/09/29/us/hurricane-ian-florida-damage.html.
Milo, R., Shen-Orr, S., Itzkovitz, S., Kashtan, N., Chklovskii, D., Alon, U., 2002. Network Motifs: Simple Building Blocks of Complex Networks. Science 298 (5594), 824–827.
Murnane, R.J., Elsner, J.B., 2012. Maximum wind speeds and US hurricane losses. Geophys. Res. Lett. 39 (16), n/a-n/a.
Musinguzi, A., Akbar, M.K., 2021. Effect of Varying Wind Intensity, Forward Speed, and Surface Pressure on Storm Surges of Hurricane Rita. J. Mar. Sci. Eng. 9 (2), 128.
Newman, M., 2018. Networks. Oxford University Press, New York, NY, USA.
NOAA. (2022). *Hurricane Ian's Path of Destruction*. NESDIS. https://www.nesdis.noaa.gov/news/hurricane-ians-path-of-destruction.
Park, S., Zhong, R.R., 2021. Pattern Recognition of Travel Mobility in a City Destination: Application of Network Motif Analytics. J. Travel Res. 61 (5), 1201–1216.
Petkova, E.P., Beedasy, J., Oh, E.J., Sury, J.J., Sehnert, E.M., Tsai, W.-Y., Reilly, M.J., 2017. Long-term Recovery From Hurricane Sandy: Evidence From a Survey in New York City. Disaster Med. Public Health Prep. 12 (2), 172–175.
Rafferty, J., 2022. Hurricane Ian | Deaths, Damage, & Facts | Britannica. Www.britannica.com. https://www.britannica.com/event/Hurricane-Ian-2022.
Rajput, A.A., Mostafavi, A., 2023. Latent sub-structural resilience mechanisms in temporal human mobility networks during urban flooding. Sci. Rep. 13 (1), 10953.
Roy, K.C., Cebrian, M., Hasan, S., 2019. Quantifying human mobility resilience to extreme events using geo-located social media data. EPJ Data Sci. 8 (1).
Sangha, K.K., Russell-Smith, J., Evans, J., Edwards, A., 2020. Methodological approaches and challenges to assess the environmental losses from natural disasters. Int. J. Disaster Risk Reduct. 49, 101619.
Schneider, C.M., Belik, V., Couronné, T., Smoreda, Z., González, M.C., 2013. Unravelling daily human mobility motifs. Journal of the Royal Society Interface 10 (84), 20130246.
Solmaz, G., Turgut, D., 2017. Modeling pedestrian mobility in disaster areas. Pervasive Mob. Comput. 40, 104–122.
Song, X., Zhang, Q., Sekimoto, Y., Shibasaki, R., Yuan, N.J., Xie, X., 2016. Prediction and Simulation of Human Mobility Following Natural Disasters. ACM Trans. Intell. Syst. Technol. 8 (2), 1–23.
Su, R., McBride, E.C., Goulias, K.G., 2020. Pattern recognition of daily activity patterns using human mobility motifs and sequence analysis. Transport. Res. Part C: Emerg. Technol. 120, 102796.
Tang, J., Zhao, P., Zi-tong, G., Zhao, H., Huang, F., Li, J., Chen, Z., Yu, L., Chen, J., 2023. Resilience patterns of human mobility in response to extreme urban floods. Natl. Sci. Rev. 10 (8).
Tanim, S.H., Wiernik, B.M., Reader, S., Hu, Y., 2022. Predictors of hurricane evacuation decisions: A meta-analysis. J. Environ. Psychol. 79, 101742.

Wang, Q., & Taylor, J. E. (2016). Diffusion and Simulation of Human Mobility Using Online Network Data to Examine Mobility Constraints. *Construction Research Congress 2016*.
Wang, J., Hu, Y., Duan, L., Michailidis, G., 2024. Analysing and visualising mobility vulnerability and recovery across Florida neighbourhoods: a case study of Hurricane Ian. Reg. Stud. Reg. Sci. 11 (1), 384–386.
Wang, Q., Taylor, J.E., 2014. Quantifying Human Mobility Perturbation and Resilience in Hurricane Sandy. PLoS One 9 (11), e112608.
Wang, Q., Taylor, J.E., 2015. Resilience of Human Mobility Under the Influence of Typhoons. Procedia Eng. 118, 942–949.
Wang, Y., Taylor, J.E., 2018. Coupling sentiment and human mobility in natural disasters: a Twitter-based study of the 2014 South Napa Earthquake. Nat. Hazards 92 (2), 907–925.
Wang, Y., Wang, Q., Taylor, J.E., 2017. Aggregated responses of human mobility to severe winter storms: An empirical study. PLoS One 12 (12), e0188734.
Washington, V., Guikema, S.D., Mondisa, J.-L., Misra, A., 2024. A data-driven method for identifying the locations of hurricane evacuations from mobile phone location data. Risk Anal. 44 (2).
Yabe, T., Jones, N.K., Rao, P.S.C., Gonzalez, M.C., Ukkusuri, S.V., 2022. Mobile phone location data for disasters: A review from natural hazards and epidemics. Comput. Environ. Urban Syst. 94, 101777.
Yum, S., 2021. The effects of Hurricane Dorian on spatial reactions and mobility. Nat. Hazards 105.
Zhai, A.R., Jiang, J.H., 2014. Dependence of US hurricane economic loss on maximum wind speed and storm size. Environ. Res. Lett. 9 (6), 064019.
Zhang, D., Huang, J., Li, Y., Zhang, F., Xu, C., He, T., 2014. Exploring human mobility with multi-source data at extremely large metropolitan scales. Proceedings of the 20th Annual International Conference on Mobile Computing and Networking -. MobiCom '14.
Zhang, X., Li, N., 2022. Characterizing individual mobility perturbations in cities during extreme weather events. Int. J. Disast. Risk Reduction 72, 102849.